Volume 4
Number 1
January 2026
Pages 1–614

RSC Sustainability

rsc.li/rscsus

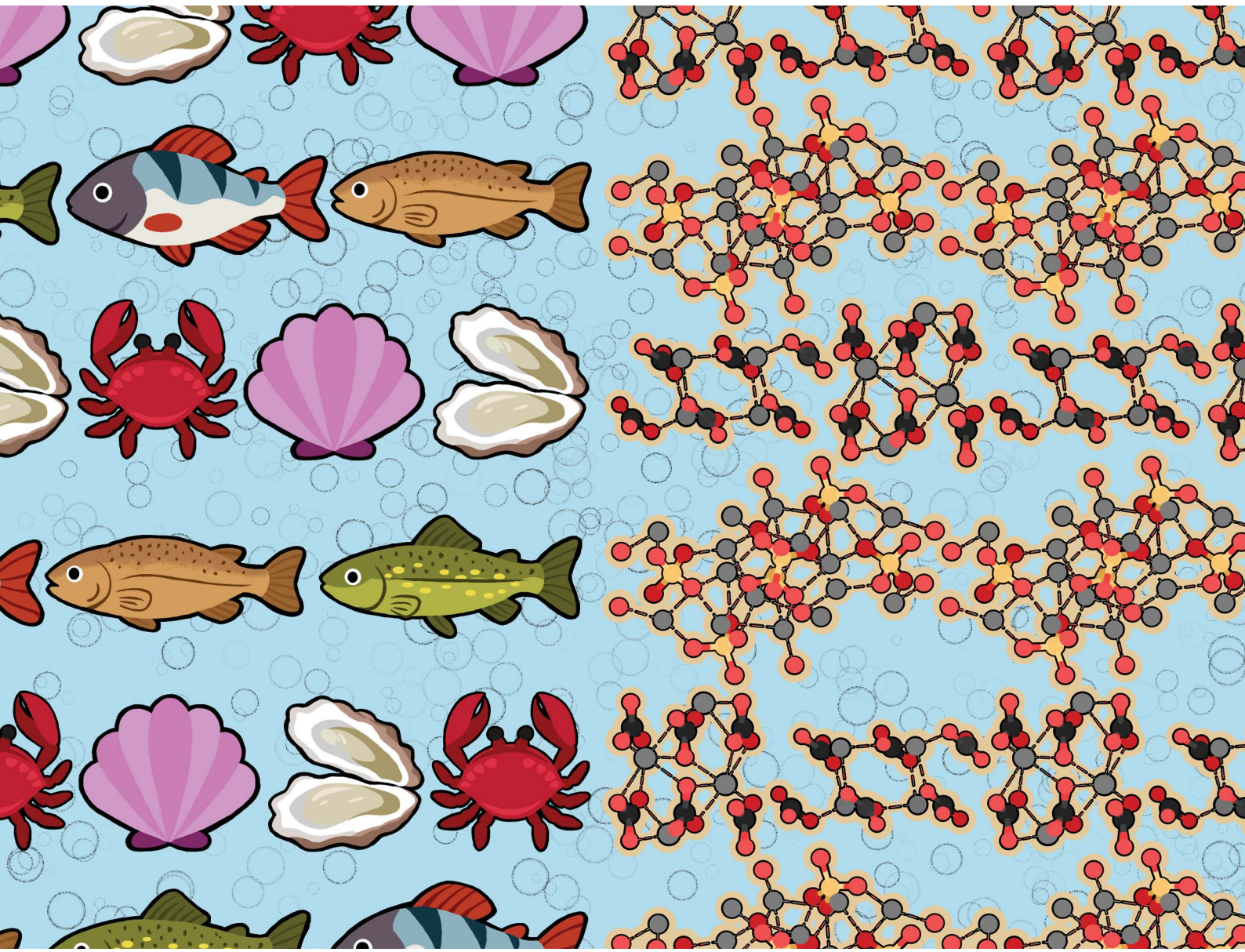

ISSN 2753-8125

ROYAL SOCIETY OF CHEMISTRY

CRITICAL REVIEW

Francesca M. Kerton *et al.*

Accessing biominerals from by-products wasted by the seafood processing industry

RSC Sustainability

ROYAL SOCIETY OF CHEMISTRY

CRITICAL REVIEW

View Article Online
View Journal | View Issue

Check for updates

Cite this: *RSC Sustainability*, 2026, **4**, 28

Accessing biominerals from by-products wasted by the seafood processing industry

Sarah Boudreau,[a] Edmond Lam [b] and Francesca M. Kerton *[a]

Due to the global population's significant growth, the demand for seafood has increased exponentially over the last century. This has led to the generation of large amounts of inedible by-products from the seafood processing industry from a multitude of marine organisms, including finfish, mollusks, and crustaceans. In this review, the potential extraction and application of biominerals from waste bones and shells originating from the seafood processing industry are discussed. Existing reviews on fishery by-products often highlight only the potential of organic by-products and disregard the biominerals present. Shells always contain calcium carbonate, $CaCO_3$, in the form of either calcite or aragonite and bones are primarily made of hydroxyapatite, $Ca_{10}(PO_4)_6(OH)_2$. The conditions used in different extraction processes to isolate the mentioned biominerals and the resulting products are compared. Furthermore, we highlight the sustainability impact of sourcing natural biominerals for global applications (*e.g.*, limestone industry) as this would prevent further environmental risks caused by improper disposal. Bio-derived minerals have also been used in other applications, such as environmental remediation and biomedicine. For calcium carbonate, the use of raw shells, their transformation to calcium oxide, CaO, and the production of precipitated calcium carbonate are presented. Next, we present in detail the isolation of hydroxyapatite from fish bones and scales, its transformation to other biphasic calcium phosphates, and its applications. The review concludes with a discussion on the strengths, weaknesses, opportunities, and threats to accessing biominerals wasted by the seafood processing industry.

Received 29th June 2025
Accepted 7th October 2025

DOI: 10.1039/d5su00527b

rsc.li/rscsus

Open Access Article. Published on 10 ottobre 2025. Downloaded on 09/05/2026 05:18:07.
This article is licensed under a Creative Commons Attribution-NonCommercial 3.0 Unported Licence.

Sustainability spotlight

Seafood is a global requirement as an important source of protein as the human population grows significantly (UN SDG2). Currently, the seafood processing industry relies on landfill and/or ocean disposal to manage the generated by-products, but this had led to greenhouse gas emissions (UN SDG13), groundwater contamination (UN SDG6 and UN SDG15), eutrophication, and acidification (UN SDG14). The biominerals present offer the potential for the seafood processing industry to create other higher-value products for consumers, a step towards achieving a circular economy (UN SDG8, UN SDG9, and UN SDG12). Sustainable processes exist in the literature to isolate biominerals from bones and shells of aquatic organisms (UN SDG11) which have then been used in multiple applications, including biomedicine (UN SDG3), environmental remediation, and catalysis.

1. Introduction

Seafood is a necessary source of protein globally and its production has increased significantly in the last century to meet the demands of the growing human population.[1,2] For example, in 1961 a person would consume on average 8.96 kg of seafood,[3] but that has increased to 20.25 kg in 2020.[3] Therefore it is not surprising that global seafood production has increased by nearly 11 000% from 1961 (1.96 million tonnes) to 2020 (214 million tonnes).[4] The countries that consume the most fish are those that do not necessarily have access to food from land-based livestock. The Maldives consumes the greatest amount with 87.30 kg per person per year,[3] followed by Iceland, Macao, and Kiribati.[3] Despite not being the largest consumers of fish, developing countries in Africa and Asia have experienced the greatest increase in seafood consumption. For example, Niger has seen the largest overall increase among all countries with an increase of over 3000% in seafood consumption while Rwanda, Nepal, and Iran have also seen significant increases of ~2400–2600%.[3]

Technological advances have contributed to the increased production of seafood. Historically, the only method of supplying fish and shellfish was by harvesting seafood directly from the ocean, from the place in which it was naturally grown, otherwise known as "capture fisheries".[3,5] However, since the 1980s, the global production from industrial capture fisheries has remained relatively stable at 90–95 million tonnes annually,[5] and is limited by the ecosystems and legislation to control over-fishing. In many regions, the quantity of fish caught by industrial vessels has been declining due to geopolitical and/or

[a]*Department of Chemistry, Memorial University of Newfoundland, St. John's, NL, Canada. E-mail: fkerton@mun.ca*

[b]*Green Chemistry Institute, American Chemical Society, Washington, DC, USA*

© 2026 The Author(s). Published by the Royal Society of Chemistry

Open Access Article. Published on 10 ottobre 2025. Downloaded on 09/05/2026 05:18:07. This article is licensed under a Creative Commons Attribution-NonCommercial 3.0 Unported Licence.

commercial dynamics. Furthermore enormous progress has been achieved in aquaculture over recent decades.[6,7] According to the Food and Agriculture Organization (FAO) of the United Nations (UN), aquaculture is defined as "the farming of aquatic organisms including fish, mollusks, crustaceans, and aquatic plants".[6,8] It was developed as a method to continue producing seafood products while alleviating some pressure on capture fisheries. In fact, aquaculture produced 123 million tonnes of seafood in 2020, surpassing quantities harvested *via* capture fisheries for the first time.[4] Finfish species represent the majority of aquaculture production and account for 46.9% of processing, followed by algae (28.6%), mollusks (14.5%), crustaceans (9.2%), and other aquatic animals (0.9%).[9] Aquatic organisms that are considered as the major aquaculture species by the FAO are listed in Table 1.

The seafood processing industries are critical for global food security, but face sustainability challenges. Industrial capture fisheries rely on fishing vessels that emit significant quantities of CO_2 (ref. 10) and can result in species depletion through overfishing. The industrial capture fish industry also causes food loss, waste, and ocean pollution during harvesting because management often encourages disposal of fish at sea (especially bycatch *i.e.* capture of unintended species),[5] and fishing gear can be abandoned, lost, or discarded.[5] Abandoned fishing gear has numerous environmental consequences including the introduction of microplastics and toxins into feed webs, habitat degradation, and the spread of invasive alien species.[11] While aquaculture was developed to overcome some of these challenges, it has also led to unintended problems that have been amplified with significant growth in this sector.† A lot of seafood is wasted due to poor harvesting practices that contribute to diseases that can cause entire pens of fish to die.[5,12] Some of the fish can potentially escape the pens and interact with local species, altering the environment and also affecting the genetics of wild fish that are protected as species at risk. If some of the escaped fish are sick, they can spread disease,[3] further affecting the local environment. Additionally, some companies have taken advantage of aquaculture and have attempted to breed too many fish in one area, thus creating anoxic zones and affecting local wildlife. Aquaculture has the potential to contribute to many of the UN's Sustainable Development Goals if care is taken to ensure economic, environmental, and social viability.[7]

Another source of waste that has yet to be mentioned is the processing of aquatic organisms post-harvest.[13] In general, processing involves chemical and mechanical operations required to transform and also preserve seafood. The first step typically involves mechanically (frequently manually) removing the entrails (*e.g.*, gutting). Most of the time, processing takes place in a factory environment which can often be labor intensive and/or highly automated. The main objective of fish processing plants is to provide fish for human consumption and the by-products (frames, skins, viscera) are sometimes processed into secondary low-profit products such as fertilizer and less frequently into higher value nutritional supplements. Processing plants situated in remote areas face challenges regarding management of by-products because alternative uses are not economically viable nor accessible. While landfills remain the most common method of disposal, remote areas are sometimes issued permits for disposal at sea when waste cannot be feasibly sent for reprocessing or to landfills.[14] In emerging economic regions of the world and in places based on subsistence/traditional fisheries, disposal of waste at sea is most common.

Relying on landfills and oceans for the disposal of seafood discards has environmental consequences. According to the FAO, food loss and waste account for 8–10% of global greenhouse gas (GHG) emissions.[15] Landfills have a significant global warming potential (GWP) because the organic content is decomposed by bacteria through aerobic and anaerobic digestion, releasing carbon dioxide (CO_2), methane (CH_4), sulfur dioxide (SO_2), and nitrogen oxides (NO_x).[16] Discards, often containing P and N, are dumped in the ocean causing eutrophication due to the abundance of nutrients present.[17,18] Eutrophication creates algae blooms that are potentially toxic, disrupt the ecosystem, taint drinking water, and eventually result in anoxic zones.[17–19] Furthermore, once these bacteria die, they release more CO_2 and contribute to ocean acidification.[20] The ocean's decrease in pH will eventually be crucial for any capture fishery or aquaculture practice at sea because it slows the growth of fish and shellfish, thus reducing catch and harvest size.[20] Due to their contribution to global warming, seafood discards should be valorized rather than disposed of and the fishing industry should strive towards a more circular economy.[21] For example, Iceland has been making significant strides in utilizing every aspect of fish towards creating higher-value products. In 2021, 80% of all Icelandic raw materials from fish were valorized as either food or other consumer products.[22] Within Iceland, the 100% Fish Project seeks a wide range of products that could be created using every part of the fish (Fig. 1).[22–24] Other than the edible seafood products, items such as cosmetics, medicinal products, and even leather have been prepared from wasted by-products that would have historically been unsustainably wasted.[22–24]

Fish and shellfish waste offer the potential to extract many high-value compounds. Typically, researchers focus on extracting organic compounds and biopolymers from seafood waste. Fish waste has been processed into various products including collagen, non-collagenous proteins, omega-3 fatty acids, and biogas. Marine collagen is of particular interest among researchers because it is highly abundant not only in fish and sharks, but also in by-catch organisms (*e.g.*, jellyfish and sea stars – previously known as starfish) too. Collagen has been extracted from seafood waste with several processes such as chemical hydrolysis, enzymatic treatment, and fermentation using proteolytic bacteria.[25] This biogenic collagen has been used in several biomedical and pharmaceutical applications because it is biocompatible and biodegradable, and it has also been used as a food additive and incorporated into packaging materials.[25]

Other biologically active compounds, including various fatty acids, have been isolated from fish by-products. For example,

† It is thought that the origins of aquaculture date back to 3000 BC *via* the construction of artificial fish ponds in China.

Open Access Article. Published on 10 ottobre 2025. Downloaded on 09/05/2026 05:18:07. This article is licensed under a Creative Commons Attribution-NonCommercial 3.0 Unported Licence.

Table 1 Production of major aquaculture species in 2020, as reported by the FAO[9]

Group	Species	World production (10^3 t, 2020)	% of group
Finfish	Grass carp (*Ctenopharyngodon idellus*)	5791.5	10.1%
	Silver carp (*Hypophthalmichthys molitrix*)	4896.6	8.5%
	Nile tilapia (*Oreochromis niloticus*)	4514.6	7.9%
	Common carp (*Cyprinus carpio*)	4236.3	7.4%
	Catla (*Catla catla*)	3540.3	6.2%
	Bighead carp (*Hypophthalmichthys nobilis*)	3187.2	5.5%
	Carassius spp.	2748.6	4.8%
	Atlantic salmon (*Salmo salar*)	2719.6	4.7%
	Striped catfish (*Pangasianodon hypophthalmus*)	2520.4	4.4%
	Roho labeo (*Labeo rohita*)	2484.8	4.3%
	Clarias catfish (*Clarias* spp.)	1249.0	2.2%
	Milkfish (*Chanos chanos*)	1167.8	2.0%
	Tilapias nei (*Oreochromis* spp.)	1069.9	1.9%
	Rainbow trout (*Oncorhynchus mykiss*)	959.6	1.7%
	Wuchang bream (*Megalobrama amblycephala*)	781.7	1.4%
	Black carp (*Mylopharyngodon piceus*)	695.5	1.2%
	Largemouth black bass (*Micropterus salmoides*)	621.3	1.1%
	Mullets nei, (Mugilidae)	291.2	0.5%
	Gilthead seabream (*Sparus aurata*)	282.1	0.5%
	Large yellow croaker (*Larimichthys croceus*)	254.1	0.4%
	European seabass (*Dicentrarchus labrax*)	243.9	0.4%
	Groupers nei (*Ephinephelus* spp.)	226.2	0.4%
	Coho (silver) salmon (*Oncorhynchus kisutch*)	221.8	0.4%
	Japanese seabass (*Lateolabrax japonicus*)	196.9	0.3%
	Pompano (*Trachinotus ovatus*)	160.0	0.3%
	Japanese amberjack (*Seriola quinqueradiata*)	137.1	0.2%
	Barramundi (Giant seaperch, *Lates calcarifer*)	105.8	0.2%
	Red drum (*Scianops ocellatus*)	84.3	0.1%
	Subtotal of major species	**45 388.1**	**79.0%**
	Subtotal of other species	**12 072.8**	**21.0%**
	Total	**57 461.1**	**100.0%**
Algae	Japanese kelp (*Laminaria japonica*)	12 469.8	35.5%
	Eucheuma seaweed (*Eucheuma* spp.)	8129.4	23.2%
	Gracilaria seaweed (*Gracilaria* spp.)	5180.4	14.8%
	Wakame (*Undaria pinnatifida*)	2810.6	8.0%
	Nori (*Porphyra* spp.)	2220.2	6.3%
	Elkhorn sea moss (*Kappaphycus alvarezii*)	1604.1	4.6%
	Fusiform sargassum (*Sargassum fusiforme*)	292.9	0.8%
	Spiny eucheuma (*Eucheuma denticulatum*)	154.1	0.4%
	Subtotal of major species	**32 861.5**	**93.7%**
	Subtotal of other species	**2216.0**	**6.3%**
	Total	**35 077.6**	**100%**
Mollusks	Cupped oyster (*Crassostrea* spp.)	5540.3	30.7%
	Japanese carpet shell (*Ruditapes philippinarum*)	4266.2	24.0%
	Scallops nei (Pectinidae)	1746.4	9.8%
	Sea mussel (Mytilidae)	1108.3	6.2%
	Constricted tagelus (*Sinonovacula constricta*)	860.3	4.8%
	Pacific cupper oyster (*Magallana gigas*)	610.3	3.4%
	Blood cockle (*Anadara granosa*)	457.9	2.6%
	Chilean mussel (*Mytilus chilensis*)	399.1	2.2%
	Subtotal of major species	**14 898.6**	**84.0%**
	Subtotal of other species	**2843.6**	**16.0%**
	Total	**17 742.2**	**100%**
Crustaceans	Whiteleg shrimp (*Penaeus vannamei*)	5812.2	51.7%
	Red swamp crawfish (*Procambarus clarkii*)	2469.0	22.0%
	Chinese mitten crab (*Eriocheir sinensis*)	775.9	6.9%
	Giant tiger prawn (*Penaeus monodon*)	717.1	6.4%
	Giant river prawn (*Macrobrachium rosenbergii*)	294.0	2.6%
	Indo-Pacific swamp crab (*Scylla serrata*)	248.8	2.2%
	Oriental river prawn (*Macrobrachium nipponense*)	228.8	2.0%
	Green mud crab (*Scylla paramamosain*)	159.4	1.4%
	Subtotal of major species	**10 705.3**	**95.3%**
	Subtotal of other species	**531.8**	**4.7%**

© 2026 The Author(s). Published by the Royal Society of Chemistry

Open Access Article. Published on 10 ottobre 2025. Downloaded on 09/05/2026 05:18:07. This article is licensed under a Creative Commons Attribution-NonCommercial 3.0 Unported Licence.

Table 1 (*Contd.*)

Group	Species	World production (10^3 t, 2020)	% of group
	Total	**11 237.0**	**100%**
Other	Chinese softshell turtle (*Trionyx sinensis*)	334.3	31.5%
	Japanese sea cucumber (*Apostichopus japonicus*)	201.5	19.0%
	Frog (*Rana* spp.)	147.8	13.9%
	Edible red jellyfish (*Rhopilema esculentum*)	90.4	8.5%
	River and lake turtle (*Testudinata*)	49.3	4.6%
	Subtotal of major species	**823.3**	**77.5%**
	Subtotal of other species	**239.0**	**22.5%**
	Total	**1062.3**	**100%**

Dave *et al.* investigated fatty acid yields in fish oil extracted from Atlantic salmon (*Salmo salar*) using enzymes and the extracted compounds included saturated fatty acids, monosaturated fatty acids, polyunsaturated fatty acids, omega-3 fatty acids, and omega-6 fatty acids.[26] Other sustainable methods for accessing omega-3 polyunsaturated acids from waste have been reported including extraction with supercritical CO_2.[27] This oil can either be used for nutritional supplementation, or it can be used as a starting material that is further reacted to create a product with other value-added applications. This has been achieved by Laprise *et al.* by epoxidizing waste-derived fish oil followed by reaction with CO_2 to yield an oil rich in cyclic carbonate groups, which could then be converted to a non-isocyanate polyurethane material.[28] Often, a sludge remains after the oil extraction process and is viewed as a by-product,[26] but it also has potential value. Paone *et al.* described their concept of an anchovy (*Engraulis* spp.) biorefinery and in their attempts to create a fully circular process, the remaining sludge after extraction was used for the production of biogas through anaerobic digestion.[29]

Crustacean shells are also useful materials because they consist of ~40% protein, ~20–25% chitin, ~5–10% lipids, and pigments.[30] Chitin, a linear polysaccharide of *N*-acetyl-D-glucosamine, is a particularly valuable compound. While it only has a few applications as a raw material because of its hydrophobicity, it is widely used in its deacetylated form, chitosan.[31] Because chitosan is more soluble in acidic and aqueous environments, it has been used in water treatment, nutraceuticals, biomedicine, and cosmetics.[32] The standard protocol to extract chitin from crustacean shells is energy- and chemically intensive, relying on hydrochloric acid (HCl) and sodium hydroxide (NaOH) for the elimination of minerals and proteins.[32] However, Burke and Kerton have recently investigated green extraction methods for the sequential extraction of carotenoid pigments, protein, and chitin from snow crab (*Chionoecetes opilio*) shells.[33] Astaxanthin was extracted with vegetable oil, a protein powder was yielded using citric acid, and chitin was recovered using enzymes.[33] Other methods that do not rely on acids and bases to extract chitin from crustacean shells include ionic liquids,[34] deep eutectic solvents (DESs),[35] supercritical fluids,[36] and mechanochemistry.[37]

The isolation of biominerals has been less prevalent compared to organic compounds despite being present in large quantities. For example, mussel shells are made of

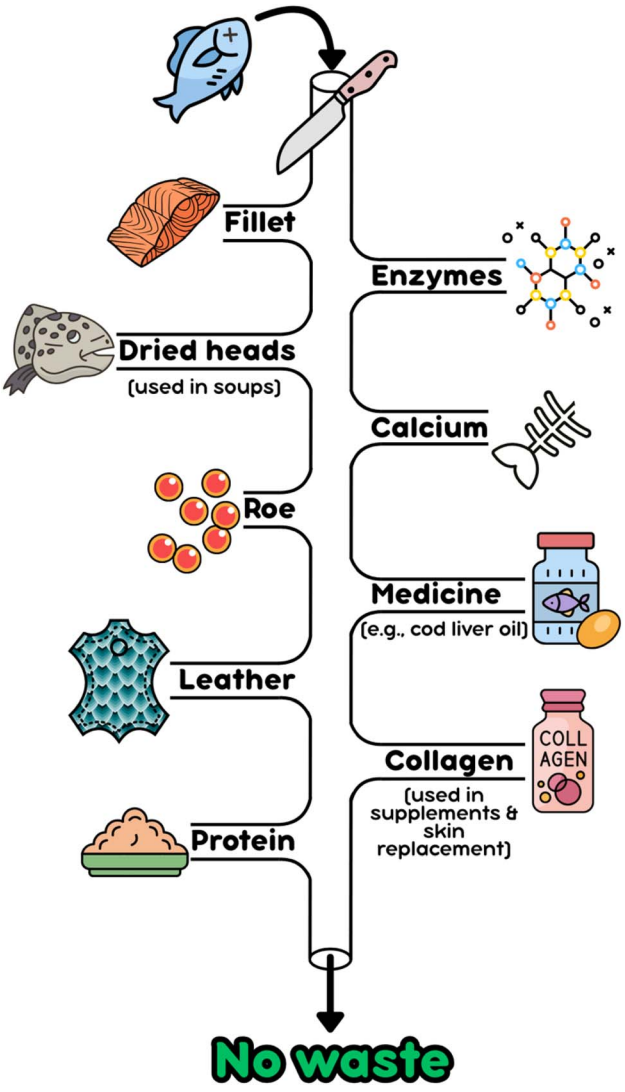

Fig. 1 Schematic representation of different value streams achieved by the Iceland Ocean Cluster's 100% Fish Project. Prepared with Canva.

Open Access Article. Published on 10 ottobre 2025. Downloaded on 09/05/2026 05:18:07. This article is licensed under a Creative Commons Attribution-NonCommercial 3.0 Unported Licence.

approximately 95% calcium carbonate ($CaCO_3$) and fish bones consist of 60% hydroxyapatite (HAP). In this review, the two biominerals most abundant in seafood waste, $CaCO_3$ and HAP, will be discussed. Marine-derived $CaCO_3$ is compared to mined limestone and exists as several polymorphs. In Section 2, $CaCO_3$ polymorphs present in shells are compared between different species of bivalves, crustaceans, and gastropods. We also touch on the transformation of biogenic $CaCO_3$ to CaO and its further processing to precipitated calcium carbonate (PCC) or HAP. In Section 3, HAP isolated from fish is compared to stoichiometric HAP and its potential benefits for biomedical applications are discussed. Finally, different isolation methods such as calcination and alkaline deproteinization are discussed for obtaining HAP by treating fish backbones and scales. Articles describing processes to isolate $CaCO_3$ or HAP from waste biomass, but with limited characterization details on the resulting minerals are omitted from this review.

2. Calcium carbonate, $CaCO_3$

It is estimated that the average American uses 40 000 lbs of new minerals annually.[38] Among these minerals, limestone makes up 71% of all crushed stone produced by the United States.[39] To be officially considered as limestone, the rock must contain >50% $CaCO_3$.[40] Limestone can be classified as impure, low purity, medium purity, high purity, and very high purity depending on the $CaCO_3$ content. Rocks with <85% $CaCO_3$ are considered impure limestone while very high purity limestone contains >98.5% $CaCO_3$.[40] While limestone itself has several applications (*e.g.*, filler in cements, concretes, plastics, paints, rubbers, and chalk),[41] it is often converted to lime, CaO.

Lime is one of the most important materials globally because it is necessary for several sectors, including steel, construction, agriculture, environmental remediation, and chemical industries.[42] For example, in 2023, 88 million tons of Portland cement were produced in the United States,[43] accounting for 95% of hydraulic cement production.[44] Portland cement is made of 60.2–68.7% CaO[45] and therefore its production is very important industrially across the world. The transformation of $CaCO_3$ to CaO is carried out *via* calcination in kilns at very high temperatures of 700–900 °C.[46–48]

Other products that can be formed from limestone: CaO, otherwise known as lime (or quicklime), can be prepared through calcination as described above. Hydrated lime (or slaked lime), $Ca(OH)_2$, is easily prepared from lime by reacting it with water.[47] PCC is $CaCO_3$ that has been artificially prepared by reacting CO_2 with a slurry of hydrated lime to produce $CaCO_3$ purer than limestone.[49] Synthesizing PCC also ensures that the $CaCO_3$ product has a definite morphology, size, and structure that may be required for specific applications.[49] For example, PCC is preferred for pharmaceutical purposes because of its high purity that comes at a relatively high cost.[40]

The limestone and lime industries are major contributors to GHG emissions, especially CO_2. According to the International Energy Agency (IEA), cement production is responsible for 7% of global anthropogenic CO_2 emissions and is the third-largest industrial energy consumer.[50] This trend is expected to rise with the growing global population, infrastructure development, and urbanisation patterns. By 2050, a 12% increase in cement production is expected. To limit the Earth's rising temperature to 2 °C, CO_2 emissions from cement manufacturing must decrease by an estimated 24%.[50] It is difficult to decarbonize the cement industry because of its inherent nature, although strides towards reducing the CO_2 emissions have been made utilizing clinker replacement, fuel alternatives, and carbon capture technologies.[46] The conversion of $CaCO_3$ to CaO will continue to be unsustainable because it is energetically demanding and releases CO_2 from both the fuel and decomposition process. Despite the difficulty in decarbonizing the limestone industry, other researchers have expressed optimism. Rissman *et al.* suggested that accepting and adopting new cement chemistries and alternative materials could help achieve a 50% reduction of industrial emissions by 2050.[51]

Another unsustainable aspect of the cement industry is obtaining limestone by mining in open quarries and blasting techniques. These methods are environmentally harmful and hazardous to the employees tasked with mining the mineral.[52] Issues that arise from mining limestone include groundwater contamination, high energy usage that generally comes from fossil fuels, creation of sinkholes, reduced biodiversity, and dust-related hazards.[53] In 2021, Stepkin *et al.* published a population health risk assessment involving communities near an industrial site for ace quarrying. They detected several pollutants in the atmosphere that have concerning toxicological characteristics, including a (1) carcinogenic effect, (2) embryotropic action, (3) gonadotropic action, (4) teratogenic action, and/or (5) a mutagenic effect.[54] To overcome the environmental and health risks associated with quarrying, $CaCO_3$ can be prepared through synthetic processes to limit environmental impact, such as precipitation/crystallization from mixing calcium and carbonate salts, but the calcium salts likely originate from the mined/quarried limestone as a feedstock.[55] A more sustainable way to obtain $CaCO_3$ is by isolating it from calcifiers: animals that rely on $CaCO_3$ to form their shells.[56] After all, most carbonate deposits that are commercially viable were created by the sedimentation of carbonate-secreting organisms many years ago.[57] This method reduces the amount of waste shells being disposed of by the fish processing industry and could thus reduce CO_2 emissions, acidification, and eutrophication.[58] Overall, extracting $CaCO_3$ from waste shellfish could help meet demands more effectively and result in an ocean-based circular economy.[59–61] Furthermore, bio-derived $CaCO_3$ is better than limestone-based $CaCO_3$ for applications that involve human use (*e.g.*, $CaCO_3$ tablets).[62] An example of this is Biocoral®, a $CaCO_3$-based coral material used as a substitute for bone grafts.[63]

$CaCO_3$ from shellfish exists as one or a combination of its three polymorphs: calcite, aragonite, and vaterite.[64] Calcite particles are found in various morphologies; it is the most thermodynamically stable polymorph and the most abundant polymorph,[65] and it has a trigonal structure with the most common form being a rhombohedron.[66,67] Aragonite particles can be needle-like[66] or plate-like nacre,[68] and occur in an orthorhombic system.[67] Vaterite particles are typically

 © 2026 The Author(s). Published by the Royal Society of Chemistry

Open Access Article. Published on 10 ottobre 2025. Downloaded on 09/05/2026 05:18:07. This article is licensed under a Creative Commons Attribution-NonCommercial 3.0 Unported Licence.

Table 2 $CaCO_3$ polymorphs present in various species of bivalves, crustaceans, and gastropods

Category	Species	Polymorphs in raw shells	Reference
Bivalves	Blue mussel (*Mytilus edulis*)	75% calcite & 25% aragonite	Murphy[68,79]
	Blue mussel (*Mytilus edulis*)	68% calcite & 32% aragonite	Cardoso[78]
	Sururu mussel (*Mytella falcata*)	94% aragonite & 6% calcite	Cardoso[78]
	Sururu mussel (*Mytella falcata*)	Mostly aragonite, little calcite	Araújo[80]
	Green mussel (*Perna viridis*)	100% aragonite	Ismail[73]
	Mediterranean mussel (*Mytilus galloprovincialis*)	Calcite & aragonite	Nam[81]
	West Indian pointed venus clam (*Anomalocardia brasiliana*)	100% aragonite	Cardoso[78]
	Spiny fileclam (*Lima lima*)	Aragonite	Anand[82]
	Brown clam (n.s.[a])	Calcite & aragonite	Aguila-Almanza[83]
	Grey clam (n.s.[a])	Calcite & aragonite	Aguila-Almanza[83]
	Ark clam (*Scarpharca subcrenata*)	Aragonite	Nam[81]
	Manila clam (*Ruditapes philippinarum*)	Mostly aragonite, little calcite	Nam[81]
	Venus clam (*Meretrix petechialis*)	Mostly aragonite, little calcite	Nam[81]
	True oyster (Ostreidae)	90% calcite & 10% aragonite	Ramakrishna[84]
	Pacific oyster (*Crassostrea gigas*)	Calcite & aragonite	Nam[81]
	Oyster (n.s.[a])	Calcite	Aguila-Almanza[83]
	Oyster (n.s.[a])	Calcite	Nguyen Quang & Ta Hong[85]
	Yesso scallop (*Patinopecten yessoensis*)	Calcite & aragonite	Nam[81]
	Pen shell (*Atrina pectinate*)	Calcite & aragonite	Nam[81]
	Egg cockle (*Fulvia mutica*)	Aragonite	Nam[81]
Crustaceans	Blue crab (*Callinectes sapidus*)	Calcite	Ogresta[86]
	Mediterranean green crab (*Carcinus aestuarii*)	Calcite	Ogresta[86]
	Mangrove crab (*Ucides cordatus*)	Calcite	Cardoso[78]
	Mangrove crab (*Ucides cordatus*)	Calcite	Araujo[80]
	Flower crab (*Portunus pelagicus*)	Calcite	Bayuseno[73]
Gastropods	Sea snail (*Loittiodea*)	Aragonite	Anand[82]
	Netted olive sea snail (*Oliva reticularis*)	Aragonite	Anand[82]

[a] Abbreviations – n.s., non-specified.

spherical[66] and belong to the hexagonal crystal system,[69] but there is ongoing discussion on the space group of vaterite, with several additional structural models being proposed such as monoclinic.[69] Calcite is the main polymorph of $CaCO_3$ found in limestone; therefore for specific applications it may be required to separate it from the other polymorphs present. Aragonite and vaterite are metastable polymorphs of $CaCO_3$ that readily transform to calcite,[65,66,70] especially vaterite which recrystallizes to calcite when it is dissolved in water.[64] $CaCO_3$ from shellfish waste is present in the form of calcite and/or aragonite depending on the species (Table 2), but vaterite can also be synthesized based on shell treatment (Table 5).[71–73]

Shellfish are made of two main groups of organisms: mollusks and crustaceans. Researchers have investigated waste shells from both groups as potential feedstocks for $CaCO_3$. The main difference between crustacean and mollusk shells is that while mollusk shells are made of ~95% $CaCO_3$, crustacean shells are more complex (*e.g.*, crab shells are composed of ~20–50% $CaCO_3$, Fig. 2).[74] Therefore, as a raw material, mollusk shells are exploited more than crab shells as a source of $CaCO_3$. However, some applications require treating the shells with calcination, thus decomposing the protein (and also chitin in crustaceans) in the process. In the next section, we will discuss using raw shells as a source of different $CaCO_3$ polymorphs and subsequently transforming them to CaO and PCC. It should be noted that seashells often contain Mg, Mn, Zn, Y, Cu, Sr, Ba, and Pb that can significantly influence the performance of materials.[75]

2.1. Raw shells

Raw shells from mollusks are made almost entirely of $CaCO_3$ in the form of calcite and aragonite. However, to utilize the shells, the organic residues must be removed; otherwise they will eventually decompose and result in a stench that is unwanted by seafood processing industries and surrounding communities. Herein, organic residues refer to all organic-containing material, including collagen. The process of cleaning waste shells is rarely discussed in the literature; however Murphy *et al.* optimized two enzymatic treatments to decompose the organic residues from raw and cooked blue mussel (*Mytilus edulis*) shells by using 1.0–2.0 μL g^{-1} Multifect PR 6L for 4 h at 55 °C and 6.0 μL g^{-1} Multifect 7L for 10 h at 25 °C, respectively.[76] A more recent preparation techniques used to isolate $CaCO_3$ from shells uses 55% v/v NaClO instead of enzymes to degrade the organic residues; however this process is less sustainable than using enzymes.[77] To isolate $CaCO_3$ from natural sources, calcination is typically avoided because it converts $CaCO_3$ to CaO at 800–900 °C.[78] Examples of $CaCO_3$ polymorphs that have been found in shells from bivalves, crustaceans, and gastropods are summarized in Table 2.

2.1.1. Bivalves. The $CaCO_3$ polymorphs present in raw shells of various bivalves have been investigated. In a 2015 study by Nam *et al.*, XRD was performed on eight species of bivalves.[81] They demonstrated that the presence of specific polymorphs depends on the evolutionary taxonomy of the bivalve's species (*e.g.*, shells within the same subclass have very similar

Open Access Article. Published on 10 ottobre 2025. Downloaded on 09/05/2026 05:18:07.
This article is licensed under a Creative Commons Attribution-NonCommercial 3.0 Unported Licence.

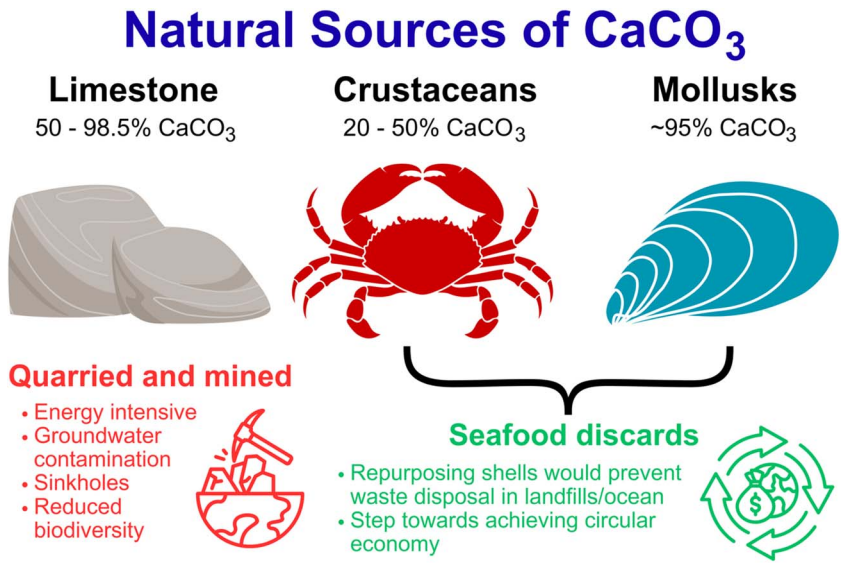

Fig. 2 Natural sources of $CaCO_3$ include limestone and calcifiers (*e.g.*, crustaceans & mollusks). Prepared with Canva.

composition). A simplified phylogenetic tree of bivalves is shown in Fig. 3.

Species that evolved within the same subclass have similar properties and contain the same $CaCO_3$ polymorph or a mixture of polymoprhs.[81] For example, bivalves belonging to the Heterodonata and Pteriomorphia subclasses are almost entirely made of aragonite. Species belonging to the Heterodonata subclass include mud-dwelling clams (*Meretrix petechialis*), Manila clams (*Ruditapes philippinarum*), and cockles (*Fulvia mutica*) while lischke (*Scarpharca subcrenata*) belongs to the Pteriomorphia subclass. The Eupteriomorphia subclass of bivalves includes species that have shells containing either calcite alone or a mixture of calcite and aragonite. The Ostreoida subclass includes species that have only calcite in their shells, such as Pacific oysters (*Crassostrea gigas*) and yesso scallops (*Patinopecten yessoensis*). A combination of calcite and aragonite is found in the shells of species from the Pterioda (*e.g.*, pen shells, *Atrina pectinata*) and Mytiloida (*e.g.*, Mediterranean mussels, *Mytilus galloprovincialis*) orders of the subclass Eupteriomorphia; however the calcite content consistently greater than that of aragonite.

Mussel shells are the most studied source of $CaCO_3$ described in the literature. Murphy *et al.* characterized the mussel shells cleaned enzymatically and showed that calcite

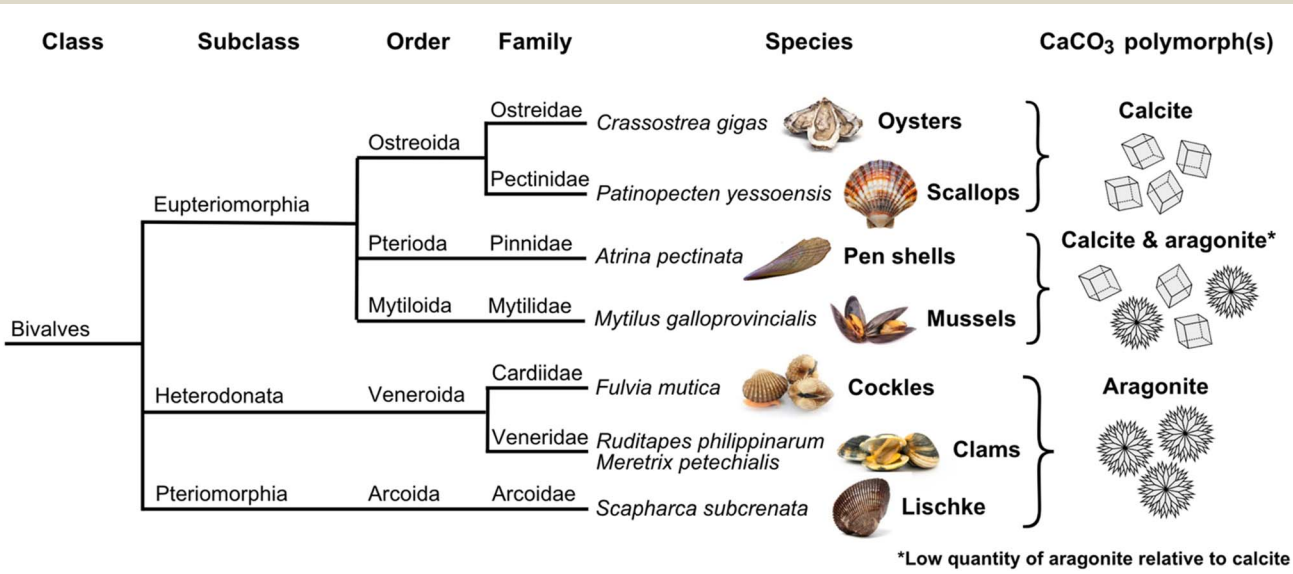

Fig. 3 Phylogenetic tree of bivalves. The subclasses Heterodonata and Pteriomorphia (*e.g.*, cockles, clams, and lischke) have shells made almost entirely of aragonite. The bivalves from the Pterioda and Mytiloida orders of the Eupteriomorphia subclass have shells made of calcite and aragonite while those from the Ostreoida order have shells made solely of calcite. These findings demonstrate that there is a relationship between $CaCO_3$ polymorphs present in shells and the evolutionary path of specific species of bivalves. Prepared with Canva.

© 2026 The Author(s). Published by the Royal Society of Chemistry

Open Access Article. Published on 10 ottobre 2025. Downloaded on 09/05/2026 05:18:07. This article is licensed under a Creative Commons Attribution-NonCommercial 3.0 Unported Licence.

and aragonite were present by XRD analysis.[68,77,79] Since that study, it has been consistently observed that blue mussel shells in particular contain a mixture of calcite and aragonite.[78] The same trend can be applied to the shells from sururu mussels, but in this case there is significantly more aragonite than calcite.[78] Interestingly, green mussel shells were observed by XRD to be composed entirely of aragonite,[87] which may be a geographical evolutionary trait.

Clam and oyster shells have also been investigated as potential feedstocks of $CaCO_3$, although they are less prevalent. Águila-Almanza *et al.* observed that clams were made of calcite and aragonite; however they did not specify the specific species of clams studied but rather categorized them based on their shell colour.[83] Cardoso *et al.* studied the shell composition of *Anomalocardia brasiliana* by XRD and reported that aragonite was the only polymorph present.[78] Oyster shells have been shown by multiple studies to consist mostly of calcite.[81,83–85]

2.1.2. Crustaceans. Compared to bivalves, there is not as much research into utilizing raw shells from crustaceans as a source of $CaCO_3$ because of the overall composition of their shells. While mussel shells are made of 95% $CaCO_3$, crab shells only contain 20–50% $CaCO_3$. Among all crustacean species (crabs, lobsters, and shrimp), crabs have been investigated the most as potential $CaCO_3$ feedstocks. Often, crab waste utilization is achieved by sequential extraction of various bio-products to yield chitin, proteins, and pigments.[32] This involves demineralization and results in other calcium-based products.[32,33] For example, Burke and Kerton described demineralizing snow crab shells using citric acid, thus yielding calcium citrate as a by-product instead of $CaCO_3$.[33] Raw crab shells from various species have been analyzed as precursors for CaO transformation (to be discussed in Section 2.2). Compared to bivalves, crab shells are much more uniform in terms of polymorph composition. Blue crab (*Callinectes sapidus*),[86] Mediterranean green crab (*Carcinus aestuarii*),[86] mangrove crab (*Ucides cordatus*),[78,80] and flower crab (*Portunus pelagicus*)[73] shells are all made solely of calcite – no aragonite was present in any of these species.

2.1.3. Gastropods. Marine gastropods, otherwise known as seasnails, are not studied often as a $CaCO_3$ source because they are not as popular for human consumption. In 2021, Anand *et al.* observed that two gastropod species, *Loittiodea* and *Oliva reticularis*, were made entirely of aragonite.[82]

2.1.4. Applications. As mentioned previously, shells can be used as a replacement for cement manufacturing and they could decrease CO_2 emitted from this industry. In Section 2.2 we describe how shells are converted to CaO, but untreated shells can also be used as aggregates in mortar and plaster – an ancient technology that continues to be used in many areas of the world.[88] A dry mortar requires three components: a binder (*e.g.*, cement), an aggregate (*e.g.*, sand), and additives (*e.g.*, fibers). $CaCO_3$ does not react with cement and therefore has potential to act as an aggregate material for this industry.[88] Mo *et al.* reviewed several examples where the properties of different types of seashells (*e.g.*, oysters, scallops, periwinkle, and mussel) were investigated as aggregates in concrete.[88] While seashells could offer a beneficial effect because of the filler effect, it should be noted that it has been reported in multiple instances that their incorporation decreases the overall strength. Therefore, the authors of the previous review focused on this specific application recommend keeping aggregate replacement below 20%. Table 3 describes some of these studies and the parameters considered.

In another study by Lertwattanaruk *et al.*, Portland cement incorporated with seashells from four species demonstrated comparable properties to those of typical plastering and masonry construction.[95] The shells were processed using wet ball milling and had average particle sizes of 13.56–29.87 μm, similar to that of Portland cement (22.82 μm). While the water requirements and setting time were improved by increasing the proportion of seashells incorporated (5–20 wt%), it should be noted that the compressive strength of mortar decreased, but the shell-based mortar continued to have adequate compressive strengths that are still higher than those needed for plastering purposes. Interestingly, the specific properties of shell-based cements were species-dependent. For example, short-necked clams (*Leukoma staminea*) and oysters decreased drying shrinkage of mortars while green mussels and cockles resulted in the opposite effect. According to the authors, mortars prepared with high volumes of short-necked clams were the best in terms of overall performance because of its relatively low mixing water requirement, good compressive strength, lower drying shrinkage, decrease in thermal conductivity, and increased setting time.

Outside of the cement industry, shell-derived $CaCO_3$ has been explored for other applications like catalysis. For example, Pasa and co-workers prepared a $CaCO_3$ catalyst from shellfish waste for biocrude production from sugarcane bagasse and ethanol.[80] Carapaces from mangrove crab and sururu mussels were crushed and sieved before being used as-is for catalysis. After 30 min at 300 °C and 10 bar N_2, biocrudes were prepared from sugarcane bagasse in high yields (72–83%). The shellfish catalysts increased the yields slightly; however there was a greater impact on the product's composition. When anhydrous ethanol was used in the presence of the catalyst, a biocrude rich in furans was observed, while hydrous ethanol instead produced ethyl esters.

Another application for shells involves dye adsorption and oil recovery. In 2020, following their work on enzymatically processing blue mussel shells,[76] Murphy *et al.* discovered that they can create an absorbent material from the shells termed "soft calcite" (SC).[79] Unlike calcite that is hard and ordered, SC has a nest-like morphology able to adsorb dyes from aqueous solutions and absorb crude oil from seawater. As mentioned previously, mussel shells are made of calcite and aragonite; however they are always present as two distinct layers. After heating the shells to 220 °C for 48 h, the outer prismatic layer (calcite) and inner nacreous layer (aragonite) can be separated mechanically. The calcite layer then undergoes two subsequent treatments with 5% acetic acid to yield SC. This novel material has a sponge-like morphology when moist, and when dried it has a cotton candy texture. It was demonstrated that SC can adsorb 1–24 wt% of common dyes (*e.g.*, crystal violet) and exhibits a significant absorption capacity of 977 g oil/g SC ± 84 g

Open Access Article. Published on 10 ottobre 2025. Downloaded on 09/05/2026 05:18:07. This article is licensed under a Creative Commons Attribution-NonCommercial 3.0 Unported Licence.

Table 3 Summary of recommendations in the literature on using seashells as aggregates and cement

Shell	Replacement	Suggested replacement level reported in the literature	Parameter(s) studied	Reference
Oyster	Fine aggregate	<20%	• Compressive strength	Yang[89]
Oyster	Fine aggregate	<50%	• Compressive strength	Eo & Yi[90]
Scallop	Fine aggregate	<40%	• Workability • Mechanical properties	Varhen[91]
Scallop	Aggregate	20–60%	• Compressive strength • Durability	Cuadrado-Rica[92]
Cockle	Cement	<15%	• Porosity	Othman[93]
Cockle	Fine aggregate	20–30%	• Compressive strength	Muthusamy[94]

for crude oil with good recyclability over ten reuse cycles. A more detailed study on the adsorption of methylene blue and safranin-O using the same materials was recently published where adsorption capacities of 1.81 and 1.51 mg g^{-1}, respectively, were achieved.[96] Since these studies, calcite from blue mussel shells has been investigated for other uses including the production of calcium acetate that can be used as a de-icer[97] or as a replacement for calcium chloride to form hydrogels.[98] Other researchers have since used mussel shells to adsorb other industrial dyes, including Eosin Y.[77]

Shells have also been explored as a possible source of $CaCO_3$ nanoparticles that can carry out drug delivery applications. In 2021, Ibiyeye and Zuki used cockle-shell-derived aragonite $CaCO_3$ nanoparticles to successfully co-deliver doxorubicin and thymoquinone to treat breast cancer.[99] The $CaCO_3$ nanoparticles were synthesized by simply grinding raw shells, adding SB-12, and then rolled on a roller mill for five days.[100] The drug-loaded aragonite nanoparticles were able to successfully destroy breast cancer stem cells and also suppress their properties. The authors describe that this combinational therapy could be useful as a potential curative strategy to manage metastasis and breast cancer recurrence.[99]

2.2. Shells as a precursor to CaO

Rather than quarrying limestone and transforming it to lime, $CaCO_3$ from shells can serve as the precursor material. The most prevalent method described in the literature to transform shells from bivalves, crustaceans, and gastropods to CaO is by calcination at temperatures above 800 °C.[78,82,101–104] $CaCO_3$ decomposes and releases CO_2 at 800 °C, resulting in CaO as the final product. A few authors, including Dampang *et al.*, use NaOH as a pre-treatment before calcination to remove organic residues;[101] however this step is probably unnecessary as proteins would decompose during calcination. A list of calcination conditions and properties of the CaO obtained are described in Table 4.

2.2.1. Applications. CaO from calcined shells have been explored as an additive in cement mortar. Compared to using $CaCO_3$ from untreated shells, calcined shells can be used as an expansive cement additive as described by Jang and colleagues.[105] The current industrial expansive additives require clinkering processes (1450 °C).[106] It should be noted that while the authors claim using calcined oyster shells could be an alternative, their process still requires 1000 °C for 3 h. Cement was substituted with 0–12 wt% calcined oyster shells and it was observed that it had a significant effect on compressive strength.[105] For example, using only 3 wt% of calcined oyster shells positively contributed to the compressive strength; however doses over 9 wt% had a significantly negative influence on the compressive strength. Therefore, while adding small quantities of calcined shell could enhance the overall properties, large quantities could lead to a lower compressive strength and loss of workability.

Shell-derived CaO has been investigated as a catalyst in the literature,[107] especially for the production of biodiesel. For example, shells from sururu, blue mussels, mangrove crab, and West Indian pointed venus clam were used to create CaO catalysts.[78] The catalyst was studied for the production of fatty acid methyl esters (FAMEs) by transesterification of soybean oil with yields of 79–94% achieved after 3.5 h. The transformation of $CaCO_3$ to CaO was achieved by calcining selected shells at 900 °C and pre-activating it with methanol for 1 h before reactions. Significantly different results were achieved depending on the shell which the CaO was derived. CaO from sururu mussels had a FAME yield of 89% after 1 h, while the other catalysts had less than a 50% yield in the same time period. The sururu CaO was investigated further, producing FAME yields of 91% after 3 h following four consecutive reuse cycles. While this is lower than the 96% FAME required to meet biodiesel production, it is a step towards using recycled waste materials for more sustainable biodiesel.

Pal and co-workers prepared a CaO catalyst using unspecified "used mollusk shells" as the starting material.[108] Interestingly, rather than just using calcination to transform $CaCO_3$ to CaO, the authors used a sol–gel method to produce $CaCl_2$ before hydrolyzing it to $Ca(OH)_2$ and then finally calcining it at 850 °C to yield CaO. The resulting product had a very distinct cubic morphology with an average particle size distribution of 341 nm. This catalyst was studied for the adsorption of a neutral red dye and the transesterification of cotton seed oil and methanol to biodiesel. When compared to commercial CaO, the mollusk-derived catalyst had better removal efficiency after 140 min (49 *vs.* 78%). Similar results were observed for transesterification reactions as mollusk-derived CaO had a maximum 98% biodiesel yield compared to commercial CaO which reached 79% with the same catalyst loading after 4.5 h of reaction time.

© 2026 The Author(s). Published by the Royal Society of Chemistry

Open Access Article. Published on 10 ottobre 2025. Downloaded on 09/05/2026 05:18:07. This article is licensed under a Creative Commons Attribution-NonCommercial 3.0 Unported Licence.

Table 4 Calcination conditions and properties of CaO produced from shells of various species of shellfish since 2020

Species	Calcination conditions	CaO properties	Reference
Blue mussel (*Mytilus edilus*)	900 °C for 3 h	Irregular morphology, diameter <5 μm	Cardoso[78]
Sururu mussel (*Mytella falcata*)	900 °C for 3 h	Irregular morphology, diameter <2 μm	Cardoso[78]
Mussel (n.s.[a])	950 °C for 4 h	Irregular morphology, diameter <10 μm	Nasir & Hazri[102]
West Indian pointed venus clam (*Anomalocardia brasiliana*)	900 °C for 3 h	Irregular morphology, diameter >5 μm	Cardoso[78]
Spiny fileclam (*Lima lima*)	900 °C for 4 h	Spherical nanoparticles, diameter: 17–31 nm	Anand[82]
Mangrove crab (*Ucides cordatus*)	800 °C for 2 h	Agglomerated microstructures with cauliflower morphology	Rezende[103]
Mangrove crab (*Ucides cordatus*)	900 °C for 3 h	Honeycomb morphology, diameter <5 μm	Cardoso[78]
Flower crab (*Portunus pelagicus*)	1000 °C for 5 h	n.s.[a]	Wibisono[104]
Sea snail (*Loittiodea*)	900 °C for 4 h	Spherical nanoparticles, diameter: 20–34 nm	Anand[82]
Netted olive sea snail (*Oliva reticularis*)	900 °C for 4 h	Spherical nanoparticles, diameter: 5–28 nm	Anand[82]
Seashell (n.s.[a])	800–1000 °C for 2–4 h	Agglomerated irregular nanoparticles	Dampang[101]

[a] Abbreviations – n.s., none specified.

Biodiesel has also been produced from castor oil and methanol using a shell-based CaO catalyst doped with praseodymium.[109] Similarly to Cardoso *et al.*,[78] mussel shells were calcined at 950 °C for 4 h to yield CaO.[109] This was doped using praseodymium nitrate hexahydrate, $Pr(NO_3)_3 \cdot 6H_2O$ and further calcined at 700 °C to create 3–11 wt% Pr-CaO catalysts. A maximum FAME yield of 87.42% was achieved using a 7 wt% Pr-CaO catalyst with a 2.5 wt% catalyst loading and methanol to oil ratio of 8 : 1 at 65 °C for 4 h. It should be noted that compared to other methods discussed previously,[78,108] the reusability of this catalyst decreased significantly to 52.46% after four cycles because of the reduced number of active sites.[109] While doping CaO with praseodymium improved the FAME yield by 7% when compared to using only calcined mussel shells, it has a negative impact on the catalyst's reusability and therefore may be impractical industrially.

Biodiesel production by transesterification of oils is not the only reaction studied using shell-derived CaO catalysts. In 2023, Eddy *et al.* used CaO from mangrove oyster (*Crassostrea gasar*) shells as a photocatalyst for the degradation of procaine penicillin in aqueous solutions.[110] The catalyst was prepared following a similar sol–gel procedure to that of Thakur *et al.*[108] The resulting CaO nanoparticles were observed by TEM to be spherical, with an average diameter of 50 nm, but SEM showed that the size was relatively uneven and some particles were >100 μm.[110] The photocatalyst had an average band gap of 4.46 eV and an absorption maximum at 280 nm, and it successfully degraded procaine penicillin under sunlight. A maximum of 97% degradation was realized experimentally after a 2 h reaction at a pH of 12 with a drug concentration of 0.0009 M. The catalyst could be reused five times while retaining efficiency above 86%. In a similar study, bromocresol green dye was degraded with efficiencies between 68 and 89% using the same CaO catalyst from oyster shells.[111]

2.3. Transforming shells to precipitated $CaCO_3$

Precipitated $CaCO_3$ (PCC) is a purified and refined version of $CaCO_3$ that has been synthesized commercially since 1841.[112] A typical process to make PCC using limestone involves (i) mining and crushing limestone, (ii) calcination to form lime, (iii) addition of water to form calcium hydroxide, $Ca(OH)_2$, (iv) combining $Ca(OH)_2$ with CO_2 to form $CaCO_3$, and (v) drying the slurry to yield PCC (eqn (1)).[113] Other reactions that produce PCC include the lime soda process (eqn (2)) and the calcium chloride process (eqn (3)).[112]

$$Ca(OH)_2 + CO_2 \leftrightarrow CaCO_3 + H_2O \quad (1)$$

$$Ca(OH)_2 + Na_2CO_3 \leftrightarrow CaCO_3 + 2NaOH \quad (2)$$

$$CaCl_2 + Na_2CO_2 \leftrightarrow CaCO_3 + 2NaCl \quad (3)$$

$CaCO_3$ produced *via* PCC processes is purer than limestone and a specific polymorph formation can be achieved – including vaterite.[70] Limestone often contains impurities such as silica and clay (Si, Al, Fe, and Mg)[114] that are avoided by using it as a precursor rather than a direct source of $CaCO_3$. Meanwhile, $CaCO_3$ must have a purity of >99% to be considered PCC.[112] Furthermore, the average size and distribution of particles formed by crushing limestone are much larger than PCC where nanoparticles can be synthesized.[70] For specific applications, such as filler pigments, PCC must be <2 μm.[112] This makes PCC superior to limestone for the preparation of impact resistant plastics and oil absorption.

As mentioned in Section 2.2, shells can also act as a source of CaO by calcining them at high temperatures to decompose $CaCO_3$. Therefore, they can be used as a precursor to synthesize PCC instead of relying on mined limestone. First, the shells are calcined at 800–1000 °C for several hours to yield CaO.[71–73,84,115] After calcination, CaO can be treated with HNO_3 before being injected with CO_2.[71,72] For example, Prihanto *et al.* reported treating CaO with HNO_3 to form an acidic solution of Ca^{2+} ions, and the pH was then increased using NH_4OH, and the desired PCC product was formed by CO_2 injection into the $Ca(NO_3)_2$ solution.[71] Other methods report that CaO becomes hydrated to form $Ca(OH)_2$ during storage by absorbing water,[73] or the CaO is directly treated with water.[84]

Open Access Article. Published on 10 ottobre 2025. Downloaded on 09/05/2026 05:18:07. This article is licensed under a Creative Commons Attribution-NonCommercial 3.0 Unported Licence.

Table 5 Synthesis methods and properties of PCC from various species of shellfish since 2017[a]

Species	PCC process	Polymorph(s)	Reference
Green mussel (*Perna viridis*)	(1) Calcined at 900 °C for 5 h (2) 2 M HNO_3 (3) pH adjusted to 11 with NH_4OH (4) Injected with CO_2 (0.25 L min^{-1}) until pH reached 7 (5) Filtered and dried	55.20% vaterite 44.80% calcite	Prihanto[71]
Green mussel (*Perna viridis*)	(1) Calcined at 800–900 °C for 5 h (2) 2 M HNO_3 at 60 °C for 30 min (3) pH adjusted to 12 with NH_4OH (4) Injected with CO_2 (5) Washed until pH reached 7 (6) Calcined at 800–900 °C for 5 h	91.26–92.16% vaterite 7.84–8.74% calcite	Ismail[72]
Green mussel (*Perna viridis*)	(1) Calcined at 900 °C for 5 h (2) Absorbed moisture during storage to form $Ca(OH)_2$ (3) 0.6 M $MgCl_2$ for 0.5–2 h (4) Injected with CO_2 (50 mL min^{-1}) until pH reached 7 (5) Filtered and dried	0.5 h stirring: 100% calcite 1 h stirring: 67.1% calcite and 32.9% aragonite 1.5 h stirring: 75.4% calcite and 24.6% aragonite 2 h stirring: 60.6% calcite, 10.0% aragonite, and 29.4% brucite	Irfa'i[115]
True oyster (Ostreidae)	(1) Calcined at 1000 °C for 2 h (2) Hydrated with H_2O (40 g L^{-1}) at 80 °C for 1 h (3) 0.6 $MgCl_2$ at 80 °C for 3 h (4) Injected with CO_2 (50 mL min^{-1}) (5) Filtered and dried	Aragonite	Ramakrishna[84]
Flower crab (*Portunus pelagicus*)	(1) Calcined at 900 °C for 5 h (2) 2 M HNO_3 at 60 °C for 30 min (3) Washed until pH reached 7 (4) Injected with CO_2 (5) Filtered and dried	Mostly vaterite Aragonite Very low amount of calcite	Bayuseno[73]

[a] Abbreviations – PCC, precipitated calcium carbonate.

One of the main advantages of using PCC rather than $CaCO_3$ is that the polymorph formation can be controlled. Naturally-derived $CaCO_3$ obtained in bulk is sometimes observed as mixture of calcite and aragonite particles with a wide particle size distribution of microparticles and nanoparticles. However, by modifying the conditions of the carbonation reaction to form PCC from $Ca(OH)_2$, the polymorph content can be tailored. Ramakrishna *et al.* studied the favourable formation of aragonite by optimizing the reaction conditions, such as the presence of $MgCl_2$, the temperature, and the time.[84] When using less than 0.1 M $MgCl_2$, calcite makes up 80% of the PCC formed; however at 0.2 M, Mg^{2+} ions start to incorporate into the Ca^{2+} ion sites of the calcite lattice to form magnesium calcite. At higher concentrations, 0.3 M, aragonite makes up 90% of the product, and at 0.6 M it makes up 100% of the PCC formed. The optimal temperature for the carbonation reaction was determined to be 80 °C by XRD as aragonite was the only polymorph present while calcite remained in small quantities at 60 and 70 °C. Finally, a reaction time of 3 h produced solely aragonite while 2.5 and 2 h resulted in a product containing calcite and unreacted $Ca(OH)_2$. Irfa'i *et al.* also investigated polymorph formation based on the duration of treatment of $Ca(OH)_2$ from green mussels with 0.6 M $MgCl_2$ prior to CO_2 injection.[115] Stirring for 0.5 h resulted solely in calcite formation; at 1–1.5 h aragonite began to precipitate, and brucite ($Mg(OH)_2$) began to form when reacted for 2 h. Some examples of PCC processes and the resulting polymorphs formed are summarized in Table 5.

3. Hydroxyapatite (HAP), $Ca_{10}(PO_4)_6(OH)_2$

HAP is an inorganic mineral that makes up 60% of human bones[116] and has been used extensively in biomedicine because of its biocompatibility,[117] non-toxicity,[118] and osteoconductivity.[119] Some examples include its incorporation into drug carriers,[120] surface coatings,[121] anti-tumour drugs,[122,123] and composites.[120] HAP has also been applied in dentistry for enamel remineralization and tooth restoration[123,124] because it makes up 70–80% of human dentin and enamel.[125] Beyond biomedicine, HAP has also been used for the bioremediation of organic and inorganic pollutants from wastewater,[126] catalysis,[127] and energy storage materials.[128]

HAP can be synthesized through a variety of methods that can be divided into three categories: dry, wet, and high temperature.[129] Solid state and mechanochemical routes are examples of dry methods in which the precursors are mixed in

 © 2026 The Author(s). Published by the Royal Society of Chemistry

Open Access Article. Published on 10 ottobre 2025. Downloaded on 09/05/2026 05:18:07.
This article is licensed under a Creative Commons Attribution-NonCommercial 3.0 Unported Licence.

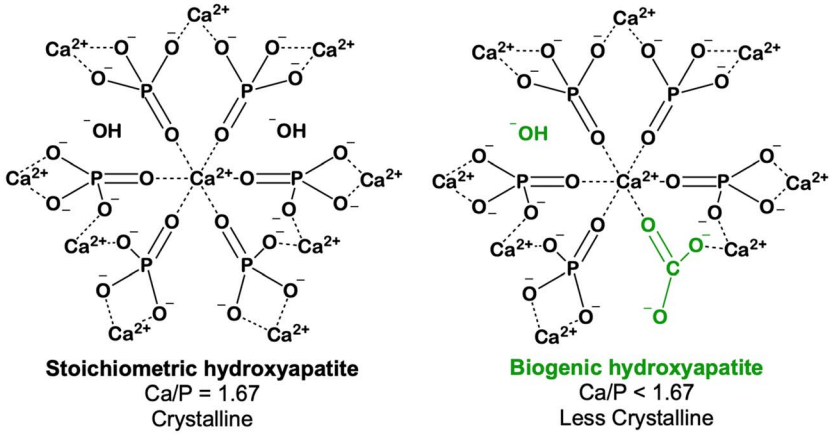

Fig. 4 Structures of stoichiometric HAP, $Ca_{10}(PO_4)_6(OH)_2$ (left) and biogenic HAP, $Ca_{10-x}(PO_4)_{6-x}(CO_3)_x$ (OH or $\frac{1}{2}CO_3)_{2-x}$ $0 \leq x \leq 2$ (right, green).

a dry form to synthesize HAP. Wet methods, including chemical precipitation, hydrothermal, and hydrolysis reactions are useful for controlling the morphology and size of the produced particles. Pyrolysis and combustion, high-temperature methods, are more rarely reported for HAP synthesis because they can result in the production of secondary aggregates, such as β-tricalcium phosphate (β-TCP).

Biogenic HAP and stoichiometric HAP do not have identical properties because of the presence of impurities. While stoichiometric HAP has the formula $Ca_{10}(PO_4)_6(OH)_2$ with a Ca/P ratio of 1.67, biogenic HAP, $(Ca_{10-x}(PO_4)_{6-x}(CO_3)_x$ (OH or $\frac{1}{2}CO_3)_{2-x}$); $0 \leq x \leq 2$, has a Ca/P ratio below 1.67 because of the presence of carbonate impurities and calcium and hydroxyl deficiencies (Fig. 4).[130] Other impurities that have been found in biogenic HAP include the following metals: Na, Mg, Cr, Co, Cu, and Sr.[131] Biogenic HAP also differs by having a lower degree of crystallinity, thus making it a more amorphous material. Stoichiometric HAP continues to be used for biomedical applications although biogenic HAP may prove to be superior because it is more biomimetic compared to the stoichiometric HAP. Stoichiometric HAP lacks the required carbonate substitutions that are critical for bones' growth, strength, and physiology. It is also a challenge to synthesize biomimetic HAP through a bottom–up process because the surface of biological apatite is rarely smooth and it contains many defects that affect crystallinity, crystal morphology, solubility, and thermal stability. Furthermore, some biomedical applications require HAP with

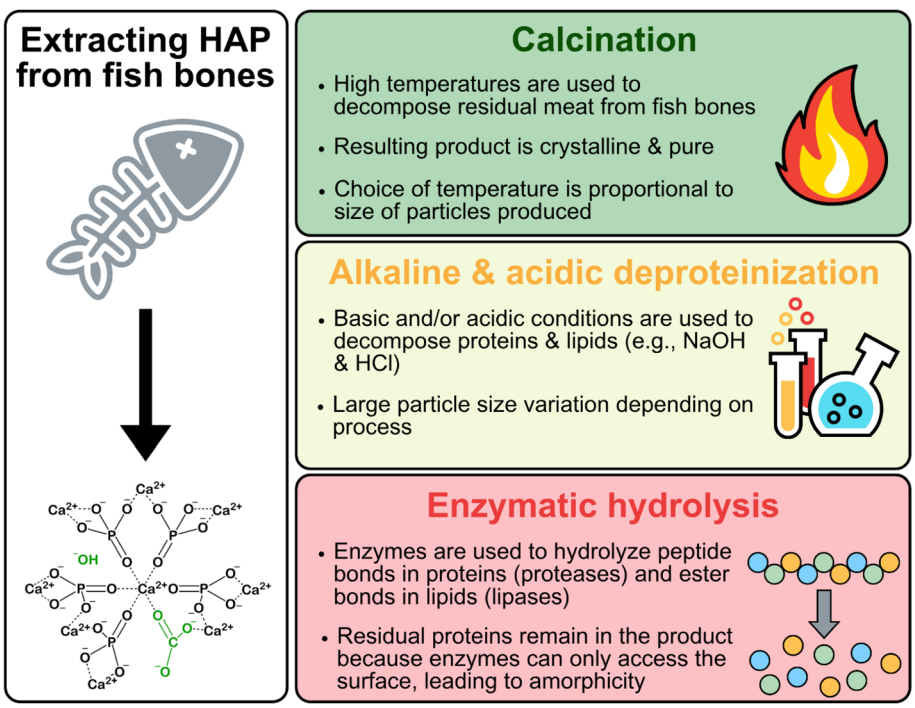

Fig. 5 Extraction techniques to isolate HAP from waste fish discards. Prepared with Canva.

Open Access Article. Published on 10 ottobre 2025. Downloaded on 09/05/2026 05:18:07. This article is licensed under a Creative Commons Attribution-NonCommercial 3.0 Unported Licence.

low crystallinity, such as cell bone regeneration because it is more biosorbable.[132]

Instead of synthesizing biomimetic HAP, this material can be obtained by isolating biogenic HAP from by-products of the seafood processing industry. Shells can be utilized as calcium precursors for HAP synthesis through bottom–up processes by converting the $CaCO_3$ in shells to CaO through calcination. The CaO can then be converted to HAP by reaction with a phosphate precursor (*e.g.*, H_3PO_4 and $NH_4H_2PO_4$).[133] Cuttlefish bones, which are made of $CaCO_3$, have also been investigated to synthesize HAP by replacing the carbonate with a phosphate to preserve the porous $CaCO_3$ structure (note: despite the name, cuttlefish are mollusks).[134] Fish bones remain the most extensively researched source of HAP, followed by scales. Several forms of fish-based biomass can be exploited to directly isolate HAP, primarily bones, scales, and teeth.

3.1. Bones

As animal species evolved from primitive organisms, the existing exoskeletons based on $CaCO_3$ were replaced with apatite-containing endoskeletons.[135] HAP has been isolated from the bones of many species of fish, ranging from sardines to tuna, and there are no obvious differences in HAP content reported between species. There are three broad processes that have been reported in the literature to remove the organic residues from the discards to yield clean bones as a source of HAP: calcination, alkaline/acidic deproteinization (AAD), and enzyme hydrolysis (Fig. 5).

3.1.1. Calcination. Calcination is the most reported method in the literature to remove organic residues from waste fish by-products to produce clean bones. This process involves heating the waste to high temperatures for several hours (*e.g.*, 1200 °C for 6 h)[136] in the presence of oxygen. It is a relatively simple method that does not require extensive sample preparation. Fish bones have been directly calcined as-is without pre-treatment (other than drying) in several studies.[137,138] Boiling the fish waste ahead of calcination for a few hours is a common pre-treatment step prior to calcination; however as demonstrated in some studies, it is not essential.[138–140] Furthermore, some methods report treating the by-products with acetone[141] or sodium hydroxide[142] as an additional (but not necessary) pre-treatment step. Grinding the fish bones (*e.g.*, in mortar or ball-mill) is often performed before calcination,[139–141,143–148] but this can be performed before or after exposing the fish bones to high temperatures (Table 6).

The choice of temperature has an impact on the HAP-containing material produced. In most studies reported to date, a range of temperatures up to 1200 °C have been explored. For example, Pal *et al.* studied the impact of different temperatures to treat barramundi (*Lates calcarifer*) waste by heating it to 200, 400, 800, 1,000, and 1200 °C with a heating ramp of 5 °C min^{-1} and holding it isothermally for 1 h.[149] By XRD analysis, it was observed that the crystallinity of the product increases depending on the chosen temperature. The samples treated at 200 and 400 °C were amorphous; however those treated at 800 °C had increased crystallinity of 80.8%. The crystallinity further increased to 89.2 and 92.9% when heated to 1000 and 1200 °C, respectively. A similar trend was observed for crystallite size, which increased from 5 nm when treated at 200 °C to 63 nm at 1200 °C. Similar results were achieved by Modolon *et al.* when they calcined tilapia (*Oreochromis niloticus*) bones at 600, 900, and 1200 °C for 2 h, observing crystallinities of 39.5, 98.3, and 99.6% and crystallite sizes of 14.4, 85.8, and 95.0 nm, respectively.[150]

At higher calcination temperatures, biphasic calcium phosphates (BCPs) are formed from the decomposition of HAP, including β-TCP and/or α-tricalcium phosphate (α-TCP).[151] This was reported by Castilho and co-workers after calcining black scabbardfish (*Aphanopus carbo*) bones at 400, 600, 800, and 1000 °C for 4 h, resulting in samples consisting of 0, 17.5, 29.7, and 40.1% β-TCP, respectively.[139] The formation of β-TCP is inconsistent across species. For example, Permatasari *et al.* observed that houndfish (*Tylosurus crocodilus*) bones calcined at 1000 °C for 4 h formed β-TCP while milkfish (*Chanos chanos*) and walking catfish (*Clarias batrachus*) did not.[140] This ultimately resulted in houndfish having much lower crystallinity (67.2%) compared to milkfish (98.3%) and walking catfish (95.0%).

The choice of calcination temperature also impacts size and morphology of BCP particles. In general, particles created at lower temperatures are smaller but less regular than those prepared at higher temperatures. For example, Carella *et al.* calcined round sardinella (*Sardinella aurita*) for 1 h at 300, 600, and 900 °C.[152] The sample calcined at 300 °C had an aligned arrangement of char that remained from the incomplete combustion of organic matter, but the size of individual particles could not be established. At 600 °C, the particles were agglomerated and spherical with a diameter of 50–100 nm. When the temperature increased to 900 °C, the particle size increased drastically to 0.20–2.0 μm with rod shape geometry. Interestingly, the morphology of BCP particles from fish bones differs across studies. Mamun *et al.* calcined tilapia and surma (*Katsuwonus pelamis*) at 900 °C for 2 h and both species resulted in agglomerated spherical particles with diameters less than 1 μm.[148] Adam and co-workers reported that black tilapia (*Oreochromis placidus*) waste produced crystal plate-like particles that are 0.5–4 μm in diameter.[153] Finally, Renda *et al.* observed that calcining tambaqui (*Colossoma macropopum*) at 900 °C for 2 h yielded cubic particles with an average diameter of 620.2 nm.[144] More details regarding calcination procedures, including the Ca/P ratio, crystallinity, and size of yielded particles, are summarized in Table 6. Processes reported without sufficient characterization information have been omitted from the table.[137,138,154–159]

3.1.2. Alkaline and acidic deproteinization (AAD). Deproteinization under acidic or basic conditions can remove protein residues from the waste fish frames. HCl and/or NaOH are typically used at concentrations between 0.1 and 1 N; however these processes often involve another treatment step to achieve the desired product, such as the use of more concentrated NaOH. Approaching this from a green standpoint, the use of acids and bases at high concentrations is undesirable because they pose a safety risk by causing severe burns and are highly

 © 2026 The Author(s). Published by the Royal Society of Chemistry

Open Access Article. Published on 10 ottobre 2025. Downloaded on 09/05/2026 05:18:07.
This article is licensed under a Creative Commons Attribution-NonCommercial 3.0 Unported Licence.

Table 6 Review of calcination treatments described in the literature to isolate BCPs[a] from fish bones since 2015

Species	Optimal treatment	Ca/P	Crystallinity	Size	Morphology	Reference
Black scabbardfish (*Aphanopus carbo*)	(1) Ground with a hand mill (2) Calcined at 400–1000 °C for 4 h	1.47–1.54	n.s.[a]	<100 nm	Isotropic	Ideia[139]
Milkfish (*Chanos chanos*)	(1) Crushed using a ball mill (2) Calcined at 1000 °C for 4 h	1.66	[b]98.3%	n.s.[a]	n.s.[a]	Permatasari[140]
Belida (*Chitala lopis*)	(1) Crushed to fine powder (2) Carbonized at 500 °C for 2 h	n.s.[a]	[c]26.8%	<20 μm	Rough and irregular	Lestari[143]
Walking catfish (*Clarias batrachus*)	(1) Crushed using as ball mill (2) Calcined at 1000 °C for 4 h	1.68	[b]95.0%	n.s.[a]	n.s.[a]	Permatasari[140]
Tambaqui (*Colossoma macropopum*)	(1) Briefly boiled (2) Ground with a mortar (3) Calcined at 600/900 °C for 2 h	n.s.[a]	High	481.1–721.7 nm (average 602.3 nm)/ 561.7–666.6 nm (average 620.2 nm)	Agglomerates of spherical/cubical particles	Renda[144]
Common carp (*Cyprinus carpio*)	(1) Boiled for 2 h (2×) (2) 500 °C for 2 h (3) Calcined at 800–1200 °C for 2–6 h (4) Ground with a mortar	1.53–1.73	High	<1 μm	Agglomerates of uniform polyhedral grains	Maidaniuc[136]
Mackerel scad (*Decapterus macarellus*)	(1) Boiled for several hours (2) Ground with a grinder (3) Calcined at 900 °C for 5 h	n.s.[a]	High	100–500 μm	Spherical microstructures	Ishak[145]
South Asian carp (*Gibelion catla*)	(1) Manually blended (2) Boiled for 8 h (3) 900 °C for 4 h (4) Ground with a mortar	n.s.[a]	Polycrystalline	200–260 nm	Hexagonal particles	Sathiyavimal[146]
Asian stinging catfish (*Heteropneustes fossilis*)	(1) Boiled for 1.5 h (2) Crushed into pieces (3) Calcined at 900 °C for 2 h	2.82	High	<1 μm	Agglomerated spherical particles	Moulick[147]
Surma (*Katsuwonus pelamis*)	(1) Boiled (2) Crushed (3) Calcined at 900 °C for 2 h	3.16	[d]92%	<1 μm	Agglomerated spherical particles	Mamun[148]
Nile tilapia (*Oreochromis niloticus*)	(1) Calcined at 900 °C for 8 h (2) Ball-milled for 8 h	1.66	n.s.[a]	650–2000 nm (average 1200 nm)	Agglomerates of irregular and rounded particles	da Cruz[160]
Nile tilapia (*Oreochromis niloticus*)	(1) Boiled (2) Calcined at 800 °C for 5 h (3) Ground with a herb grinder for 10 min	1.64	Low	10–25 μm	Irregular-shaped particles	Khamkongkaeo[132]
Nile tilapia (*Oreochromis niloticus*)	(1) Boiled (2) Crushed in a knife-mill (3) Ball-milled (4) Calcined at 600–1200 °C for 2 h (5) Ball-milled for 1–3 h with isopropyl alcohol	1.85–1.93	[d]39–99%	1–2 μm	Irregular particles that become bigger with temperature	Modolon[150]
Nile tilapia (*Oreochromis niloticus*)	(1) Boiled (2) Crushed into small pieces (3) Calcined at 900 °C for 2 h	2.99	[d]94%	<1 μm	Agglomerated spherical particles	Mamun[148]
Black tilapia (*Oreochromis placidus*)	(1) Boiled (2) Calcined at 800 °C	n.s.[a]	High	0.5–4 μm (average 1.2 μm)	Plate-like structure	Hubadillah[153]

© 2026 The Author(s). Published by the Royal Society of Chemistry

Open Access Article. Published on 10 ottobre 2025. Downloaded on 09/05/2026 05:18:07.
This article is licensed under a Creative Commons Attribution-NonCommercial 3.0 Unported Licence.

Table 6 (*Contd.*)

Species	Optimal treatment	Ca/P	Crystallinity	Size	Morphology	Reference
Pama croaker (*Otolithoides pama*)	(1) Boiled for 1.5 h (2) Crushed into pieces (3) Calcined at 900 °C for 2 h	2.82	n.s.[a]	<1 μm	Agglomerated spherical particles	Prosad Moulick[147]
Perch (*Perca* sp.)	(1) Boiled for 8 h (2) Calcined at 900 °C for 2 h (3) Ground with a mortar	~1.67	High	50–80 nm	Agglomerated spherical particles	Naga[161]
Round sardinella (*Sardinella aurita*)	(1) Calcined at 300–900 °C for 1 h (2) Ground and sieved (50 μm)	1.54–1.60	[e]<5–60%	50–100 nm (600 °C); 0.2–2 μm (900 °C)	Round particles (600 °C); regular and coarse rods (900 °C)	Carella[152]
Atlantic salmon (*Salmo salar*)	(1) Immersed in NaOH for 24 h (2) Calcined at 850 °C for 4 h (3) Crushed with a mortar (4) Ball-milled for 4 h	1.57	High	<5 μm	Agglomerated spherical particles	Popescu-Pelin[142]
Rabbitfish (*Siganus* sp.)	(1) Boiled (2) Boiled in water & acetone for 1 h (3) Ground with a mortar into 200-mesh powder (4) Annealed at 800–1000 °C for 2 h (5) Ball-milled for 30 min	1.696–1.876	n.s.[a]	1–5 μm	Agglomerated irregular particles	Fendi[141]
Catfish (*Siluriformes* sp.)	(1) Boiled for 4 h (2) Sintered at 900 °C for 2 h (3) Ground with a mortar and sieved (300 μm)	1.58	[d]99%	<200 μm	Irregular flower-like microstructures with petal-shaped flakes	Akpan[162]
Gilt-head bream (*Sparus aurata*)	(1) Immersed in NaOH for 24 h (2) Calcined at 850 °C for 4 h (3) Crushed with a mortar (4) Ball-milled for 4 h	1.63	High	<5 μm	Agglomerated spherical particles	Popescu-Pelin[142]
Spanish mackerel (*Tenggiri scomberomorini*)	(1) Crushed to fine powder (2) Carbonized at 500 °C for 2 h	n.s.[a]	25.6%[c]	<20 μm	Rough and irregular particles	Lestari[143]
Houndfish (*Tylosurus crocodilus*)	(1) Crushed with a ball mill (2) Calcined at 1000 °C for 4 h	1.62	[b]67.2%	n.s.[a]	n.s.[a]	Permatasari[140]

[a] Abbreviations – BCP, biphasic calcium phosphate; n.s., non-specified. [b] Crystallinity calculated using an unspecified method. [c] Crystallinity calculated using software. [d] Crystallinity calculated by comparing the intensity of the largest peak and the valley between the largest peak and first peak on the right (eqn (S1)). [e] Crystallinity calculated by comparing the sum of peaks and the area between the peaks and background (eqn (S2)).

© 2026 The Author(s). Published by the Royal Society of Chemistry

Open Access Article. Published on 10 ottobre 2025. Downloaded on 09/05/2026 05:18:07. This article is licensed under a Creative Commons Attribution-NonCommercial 3.0 Unported Licence.

reactive. Furthermore, acids and bases can pose an environmental risk if not disposed of properly. That being said, they continue to be used to isolate HAP from fish by-products. For example, Surya *et al.* described boiling sardine (*Sardinella longiceps*) bones in 2% NaOH and acetone for 1 h, followed by another treatment with 5% NaOH for 5 h at 70 °C.[163] This was then further treated with 50% NaOH at 100 °C for 1 h to yield nano-hydroxyapatite (nHAP) particles.[163] In this reaction, not only is concentrated NaOH used that is corrosive and reactive, but acetone is also employed which can generate leachates. Rather than using 50% NaOH and acetone, Nag *et al.* immersed fish bones from various fish species in 30% H_2O_2 after an initial treatment with a commercial detergent solution.[164]

Autoclaving and calcination are other treatment steps that are used in conjunction with AAD to ensure thorough removal of organic residues. Triwitono and co-workers treated fish bones from six species of fish by autoclaving them at 121 °C for 3 h before using 1 N HCl and 1 N NaOH.[165] Meanwhile, Hariani *et al.* calcined milkfish (Chanidae sp.) at 750 °C for 3 h after using 0.1 N HCl and 50% NaOH.[166] The method reported by Idowu *et al.* is quite different from others: Atlantic salmon bones were immersed in 2 M NaOH and soaked in hexane before being treated with 2.5% NaClO and finally calcined at 900 °C for 6–9 h.[167]

AAD often yields a more amorphous product, whereas calcination increases crystallinity. For example, Horta *et al.* extracted HAP from tambaqui bones with 1% NaOH and calcined a portion of these bones at 800 °C.[168] They determined that the alkaline treatment decomposed a significant amount of organic material, but calcination was required to increase the crystallinity significantly. Based on SEM observations, samples not exposed to heat were made of agglomerated, irregularly shaped nanoparticles while calcination yielded larger, more defined particles. As with calcination, the HAP particles tend to agglomerate regardless of the method of preparation and it is often difficult to compare results since some studies report the size of individual nanoparticles while others describe the size of agglomerates. Deproteinization treatments involving acids and/or bases are summarized in Table 7 but reports that did not include sufficient characterization data have been omitted.[164,169]

3.1.3. Enzymatic hydrolysis. Using enzymes is a relatively uncommon technique to isolate HAP from waste fish bones compared to calcination and alkaline/acidic deproteinization. It is the most sustainable and industry-friendly option because of the limited amounts of solvent, acid/base, and heat required for a successful process. Proteases are the most commonly studied enzymes for decomposing organic content in fish by-products, although other enzymes such as lipases and enzymatic cocktails have also been used. Fitri *et al.* used 8% papain enzyme for 10 h at 60 °C in water to treat milkfish bones; however some lipid content remained in the sample as indicated by IR data.[173] Furthermore, the product was highly amorphous based on the XRD diffractogram of the treated milkfish bones. Boudreau *et al.* overcame this challenge by using a protease, Neutrase, and a lipase, Lipozyme CALB L, simultaneously in water at 40 °C for 6 h.[174] While collagen remains present within the bone matrix, this is expected, as the enzymes do not penetrate the solid material in which the collagen is encased. Compared to Fitri *et al.*,[173] the lipid content was significantly reduced by the addition of a lipase. Boudreau *et al.* continued this research by using mechanochemistry techniques to transform the cleaned fish bone macroparticles into HAP nanoparticles for further applications.[175] Furthermore, a simplified gate-to-gate life cycle analysis (LCA) showed that using enzymes and mechanochemistry to yield HAP nanoparticles is safer for human exposure and releases significantly lower quantities of CO_2 compared to using calcination and/or AAD.[175]

To achieve a product with higher purity, Pou and co-workers calcined fish bones from horse mackerel (*Trachurus trachurus*), scorpionfish (*Scorpaena scrofa*), and Atlantic salmon at 750–950 °C for 10 h after treating them with 1% Alcalase for 4 h at 64.2 °C.[176] As expected, the extracted HAP is more crystalline and has no traces of organic residues (*e.g.*, lipids and proteins) compared to that obtained by Boudreau *et al.* because of the calcination step.[174–176] The samples calcined at 950 °C were more crystalline than those calcined at 750 °C, but higher amounts of β-TCP were also detected. Similar results were achieved by enzymatically treating catfish (*Pangasius hypophthalmus*) waste with Alcalase and calcination for 3 h at 500–900 °C.[177] As the temperature increased, partial decomposition of HAP to β-TCP also increased.

Enzymes have the potential to create a more circular economy for the seafood processing industry. As mentioned above, not only are enzymes considered green, but every aspect of the fish waste could be utilized. While the focus of this review is on the inorganic fraction of the by-products, the protein hydrolysate remaining after enzymatic treatment contains beneficial amino acids that could be incorporated into fertilizers.[178–180]

3.2. Scales

Researchers have successfully isolated HAP from waste fish scales despite having lower inorganic content (38–46%) compared to bones. While many follow processes previously reported for the treatment of bones (*i.e.*, calcination, AAD, and enzymes), other novel methods have also been used such as ultrasonic-assisted extraction (UAE) and treatment with DES. Among these methods, alkaline deproteinization is the most common treatment, followed by calcination, UAE, and finally DES. The isolated HAP is often observed as agglomerates of particles with sizes ranging from 5 nm to 167 μm. A detailed list of these methods is summarized in Table 8 but reports that did not provide sufficient characterization information are omitted.[181–184]

3.2.1. Calcination and pyrolysis. To study the impact of temperature, Ideia *et al.* calcined scale-containing skins from grey triggerfish (*Balistes capriscus*) at 400, 600, 800, and 1000 °C for 4 h.[139] Sardine (*Sardina pilchardus*) bones were also treated under the same conditions to compare the HAP obtained from bones to scales. At 400 °C, both samples were poorly crystalline; however crystallinity increased proportionally for scales and bones with temperature. Interestingly, while the bones calcined at 1000 °C were composed of 40.1 wt% β-TCP and 59.9 wt%

Open Access Article. Published on 10 ottobre 2025. Downloaded on 09/05/2026 05:18:07.
This article is licensed under a Creative Commons Attribution-NonCommercial 3.0 Unported Licence.

Table 7 Review of AAD[a] treatments described in the literature to isolate HAP from fish bones since 2018

Species	Optimal treatment	Ca/P	Crystallinity	Size	Morphology	Reference
Milkfish (*Channidae* sp.)	(1) Crushed by fast milling (2) Sieved through a 200-mesh sieve (3) Washed with 0.1 N HCl (4) Treated with 50% NaOH for 5 h at 60 °C (5) Calcined at 750 °C for 3 h	1.65	n.s.[a]	<3 μm	Irregular and agglomerated particles	Hariani[166]
Tambaqui (*Colossoma macropomum*)	(1) Boiled in water for 1 h (2) Treated with 1% NaOH at 90 °C for 5 h (3) Crushed with a mortar (4) Calcined at 800 °C	1.67	n.s.[a]	<500 nm	Defined morphology with a faceted structure	Horta[168]
Grouper (*Epinephelus* sp.)	(1) Boiled in water for 1 h (2) Autoclaved at 121 °C for 3 h (3) Crushed with a mortar (4) Soaked in 1 N HCl for 1 h (5) Centrifuged for 15 min (6) Treated with 1 N NaOH for 1 h at 100 °C (3×) (7) Neutralized with 1 N HCl and centrifuged (8) Refined with a disc mill for 1 min (9) Sieved through a 200-mesh sieve	1.44	[b]69.8%	Ave. 281.4 nm	Agglomerates of asymmetrical particles	Kusumawati[165]
Barramundi (*Lates calcarifer*)	(1) Boiled in water for 1 h (2) Boiled in 1% NaOH (3) Calcined at 650 °C for 4 h (4) Crushed with a mortar	1.845	High	Ave. 39.42 nm long, 17.15 nm wide	Spherical and rectangular particles	Le Ho[170]
Snapper (*Lutjanus* sp.)	(1) Boiled in water for 1 h (2) Autoclaved at 121 °C for 3 h (3) Crushed with a mortar (4) Soaked in 1 N HCl for 1 h (5) Centrifuged for 15 min (6) Treated with 1 N NaOH for 1 h at 100 °C (3×) (7) Neutralized with 1 N HCl and centrifuged (8) Refined with disc mill for 1 min (9) Sieved through a 200-mesh sieve	1.38	[b]71.2%	Ave. 254.7 nm	Agglomerates of asymmetrical particles	Kusumawati[165]
Whitemouth croaker (*Micropogonias furnieri*)	(1) Washed with 1 N NaOH for 24 h (2) Washed in water overnight (3) Treated with 30% H_2O_2 for 24 h (4) Calcined at 800 °C for 5 h (5) Milled	1.40	High	>10 μm	Agglomerates of asymmetrical particles	Yamamura[171]
Tilapia (*Oreochromis niloticus*)	(1) Boiled in water for 1 h (2) Autoclaved at 121 °C for 3 h (3) Crushed with mortar (4) Soaked in 1 N HCl for 1 h (5) Centrifuged for 15 min (6) Treated with 1 N NaOH for 1 h at 100 °C (3×) (7) Neutralized with 1 N HCl and centrifuged (8) Refined with disc mill for 1 min (9) Sieved through a 200-mesh sieve	1.61	[b]70.2%	Ave. 87.4 nm	Agglomerates of asymmetrical particles	Kusumawati[165]

© 2026 The Author(s). Published by the Royal Society of Chemistry

Open Access Article. Published on 10 ottobre 2025. Downloaded on 09/05/2026 05:18:07.
This article is licensed under a Creative Commons Attribution-NonCommercial 3.0 Unported Licence.

Table 7 (*Contd.*)

Species	Optimal treatment	Ca/P	Crystallinity	Size	Morphology	Reference
Catfish (*Pangasius* sp.)	(1) Boiled in water for 1 h (2) Autoclaved at 121 °C for 3 h (3) Crushed with amortar (4) Soaked in 1 N HCl for 1 h (5) Centrifuged for 15 min (6) Treated with 1 N NaOH for 1 h at 100 °C (3×) (7) Neutralized with 1 N HCl and centrifuged (8) Refined with a disc mill for 1 min (9) Sieved through a 200-mesh sieve	1.43	[b]72.2%	Ave. 239.9 nm	Agglomerates of asymmetrical particles	Kusumawati[165]
Atlantic salmon (*Salmo salar*)	(1) Boiled in water for 1 h (2) Treated with 1% NaOH (3) Calcined at 800 °C for 3 h (4) Ground in a centrifugal ball mill (5) Sieved through a 63 μm sieve	1.63	High	Ave. 122 nm	Agglomerates of grain-like particles	Bas[172]
Atlantic salmon (*Salmo salar*)	(1) Immersed in 2 M NaOH at 50 °C for 2 h (2) Ground with a crushing mill until particles were 3–4 mm long (3) Treated with hexanes for 1 h at 25 °C (4) Bleached with 2.5% NaClO for 30 min (5) Bleached with 2.5% H_2O_2 for 1 h (6) Milled with a planetary ball mill for 2.5 h (7) Sieved with a 75 mm sieve (8) Calcined at 900 °C for 6–9 h (9) Milled with a planetary mill	1.66	High	22.2–27.5 μm	Nanoparticles agglomerates into large clusters	Idowu[167]
Indian oil sardine (*Sardinella longiceps*)	(1) Boiled at 200 °C (2) Boiled with 2% NaOH and acetone for 1 h (3) Grinded with a mortar (4) Treated with 5% NaOH at 70 °C for 5 h (5) Precipitants treated with 50% NaOH at 100 °C for 1 h (6) Sieved	n.s.	Low	<5 μm	Agglomerates of asymmetrical particles	Surya[163]
Kingfish mackerel (*Scomberomorus* sp.)	(1) Boiled in water for 1 h (2) Autoclaved at 121 °C for 3 h (3) Crushed with a mortar (4) Soaked in 1 N HCl for 1 h (5) Centrifuged for 15 min (6) Treated with 1 N NaOH for 1 h at 100 °C (3×) (7) Neutralized with 1 N HCl and centrifuged (8) Refined with a disc mill for 1 min (9) Sieved through a 200-mesh sieve	1.69	[b]64.9%	Ave. 105.2 nm	Agglomerates of asymmetrical particles	Kusumawati[165]

Open Access Article. Published on 10 ottobre 2025. Downloaded on 09/05/2026 05:18:07. This article is licensed under a Creative Commons Attribution-NonCommercial 3.0 Unported Licence.

Table 7 (*Contd.*)

Species	Optimal treatment	Ca/P	Crystallinity	Size	Morphology	Reference
Tuna (*Thunnus* sp.)	(1) Boiled in water for 1 h (2) Autoclaved at 121 °C for 3 h (3) Crushed with a mortar (4) Soaked in 1 N HCl for 1 h (5) Centrifuged for 15 min (6) Treated with 1 N NaOH for 1 h at 100 °C (3×) (7) Neutralized with 1 N HCl and centrifuged (8) Refined with a disc mill for 1 min (9) Sieved through a 200-mesh sieve	1.36	[b]64.3%	Ave. 150.2 nm	Agglomerates of asymmetrical particles	Kusumawati[165]

[a] Abbreviations – AAD, alkaline and/or acidic deproteinization; n.s., none specified; Ave., average. [b] Crystallinity calculated using software.

HAP, the scales were almost entirely made of HAP (95.8 wt%). β-TCP was present in scales only at 600 °C and in much lower quantities (4.6 wt%) compared to bones. Scales also contained minerals that were not observed in bone samples such as halite, NaCl, and rhenanite, $NaCaPO_4$. Halite was present in samples calcined at 200–800 °C and decreased with increasing temperature, while rhenanite was only observed in scales treated at 600 and 800 °C. Additionally, the remaining 4.2 wt% of scales calcined at 1000 °C was attributed to magnesium oxide, MgO, and cubic trisodium phosphate, γ-Na_3PO_4. The samples were studied by SEM and particulate size increased with temperature as a consequence of grain growth due to the added energy. The scale-derived particles were consistently larger than those created from bone, regardless of temperature. Furthermore, the particles prepared had completely different morphologies. While the calcination of bones at 600 °C resulted in agglomeration of spherical particles, scales yielded rod-like particles with a hexagonal prism morphology. Also, at 800 °C, there were other particles with a secondary flower-like morphology observed in the heated skin samples, which were attributed to rhenanite.

In 2022, Rattanakam and co-workers published a study on the dissolution performance of carbon/HAP nanocomposites from tilapia scales.[194] Instead of calcining, they pyrolyzed the discards at 450, 500, 550, and 600 °C for 5 h. The final material prepared was ultimately collected on a 0.5-mm sieve prior to analysis. The Ca/P ratio of each product was significantly higher (2.43–2.50) than those observed from other thermal treatments, but this can be attributed to the fact this was a pyrolysis treatment in the presence of nitrogen rather than calcination. Without oxygen, biochar was produced from the decomposition of protein, and therefore the carbon content was high (22.6–25.6 wt%). Broad and low intensity peaks were observed in the XRD diffractograms, indicating that the products were amorphous. The authors highlighted that the crystal size of the samples did not increase proportionally with temperature, unlike calcination, because the carbon in organic residues linked to HAP could block its nucleation sites, preventing particle growth and recrystallization. The authors later noted that distinguishing between carbon and HAP particles during TEM analysis was not possible because of severe aggregation. Therefore, while pyrolysis may not increase the size of particles yielded, it does not prevent agglomeration.

3.2.2. Alkaline and acidic deproteinization (AAD). While researchers most often rely on calcination to isolate HAP from waste fish bones, AAD is much more common when treating scales because they have a higher lipid content.[199] Often these methods report using concentrated NaOH after pre-treating the scales with dilute acid or base. For example, Eswaran *et al.* used 0.1 M HCl to remove proteins from mullya garra (*Garra mullya*) scales, followed by 5% (w/v) NaOH for 7 h at 70 °C.[187] After being dried overnight and crushed using a mortar and pestle, samples were immersed in 50% (w/v) NaOH for 2 h at 100 °C for further deproteinization. Lee and co-workers followed a very similar procedure to synthesize HAP from black tilapia scales to study its adsorption efficiency for Cr(VI) removal.[191] The particles prepared from the tilapia scales were slightly larger (50–60 nm wide and 30–200 nm long)[191] than mullya garra (5–20 nm wide and 20–40 nm long).[187]

The morphology of HAP particles extracted from natural sources is still not fully understood as the same technique can provide particles with different shapes. For example, Eswaran *et al.*[187] and Injorhor *et al.*[185] followed a method very similar to that reported by Kongsri *et al.*[200] HAP from the Nile tilapia scales was in the form of hexagonal crystals with an average size of 20 nm. While the size is similar to those of other HAP particles prepared,[200] scales from mullya garra were rod-like[187] and white seabass scales had irregular morphology.[185] While Eswaran *et al.* describe grinding their scales with a mortar and pestle during their multi-step alkaline treatment,[187] the other methods do not mention any further treatment prior to characterization.[185,200] More research into the choice of mechanochemical processing method (*e.g.*, mortar and pestle, ball-milling, and planetary mill) could provide further insight into whether it has an impact on particle morphology.

© 2026 The Author(s). Published by the Royal Society of Chemistry

Open Access Article. Published on 10 ottobre 2025. Downloaded on 09/05/2026 05:18:07.
This article is licensed under a Creative Commons Attribution-NonCommercial 3.0 Unported Licence.

Table 8 Review of calcination, AAD,[a] DES,[a] and UAE[a] treatments described in the literature to isolate BCPs[a] from fish scales since 2020

Method	Species	Optimal treatment	Ca/P	Crystallinity	Particle size & morphology	Reference
AAD[a]	White seabass (*Astractoscion nobilis*)	(1) Immersed in 0.1 M HCl for 1 h (2) Treated with 5% NaOH at 60 °C for 3 h (3) Treated with 50% NaOH at 80 °C for 3 h	2.01	[b]80.99%	Size: 100–500 nm (mean: 172.9 nm)	Injorhor[185]
	Catla (*Catla catla*)	(1) Soaked in 83 mL of 1 N HCl for 30 min (2) pH raised to 11 with 6 N NaOH (3) Vacuum filtered (4) Boiled in a bag in a water bath for 30 min (5) Frozen at −80 °C overnight (6) Incubated in a hot air oven at 160 °C overnight (7) Calcined at 800 °C for 2 h	1.66	n.s.[a]	Size: <1 μm Morphology: agglomerates of needles	Buraiki[186]
	Mullya garra (*Garra mullya*)	(1) Immersed in 500 mL 0.1 M HCl (2) 250 mL 5% NaOH added and stirred at 70 °C for 7 h (3) Dried precipitates crushed using a mortar and pestle (4) Stirred in 100 mL 50% NaOH at 100 °C for 2 h	1.67	High	Size: 20–40 nm long and 5–20 nm wide Morphology: interconnected nanostructured rods	Eswaran[187]
	Rohu (*Labeo rohita*)	(1) 100 g immersed in 0.6% KOH (×2) (2) Calcined at 550–1000 °C for 3 h	1.52–1.82	n.s.[a]	Size: 1–1000 μm, mean of 155–167 μm Morphology: surface layer with bony ridges of HAP in concentric rings & an inner fibrous layer of mainly collagen	Sarkar and Das[188]
	Asian sea bass (*Lates calcarifer*)	(1) Stirred in 1 L of 0.25 M HCl for 2 h (2) Calcined at 900 °C for 3 h (3) Ground and sieved through a cloth mesh	1.67	n.s.[a]	Size: 50–150 nm Morphology: spherical agglomerates	Wu[189]
	Nile tilapia (*Oreochromis niloticus*)	(1) Soaked in 83 mL of 1 N HCl for 30 min (2) pH raised to 11 with 6 N NaOH (3) Vacuum filtered (4) Boiled in a bag in a water bath for 30 min (5) Frozen at −80 °C overnight (6) Incubated in a hot air oven at 160 °C overnight (7) Calcined at 800 °C for 2 h	2.14	n.s.[a]	Size: <1 μm Morphology: spherical agglomerates	Buraiki[186]
	Nile tilapia (*Oreochromis niloticus*)	(1) Ground into a fine powder (2) Stirred in 1 L 0.75 M NaOH at 60 °C for 5 min (3) Solid portion added to 1.3 M HCl at 60 °C for 30 min (4) 5 M NaOH added dropwise (5) Ground	2.25	Low	Size: 250–2500 nm Morphology: dense agglomerated soft morphology with high surface roughness	Rashad[190]

Open Access Article. Published on 10 ottobre 2025. Downloaded on 09/05/2026 05:18:07. This article is licensed under a Creative Commons Attribution-NonCommercial 3.0 Unported Licence.

Table 8 (*Contd.*)

Method	Species	Optimal treatment	Ca/P	Crystallinity	Particle size & morphology	Reference
	Black tilapia (*Oreochromis placidus*)	(1) Immersed in 0.1 M HCl for 12 h (2) Stirred in 5% NaOH at 70 °C for 5 h (3) Treated with 50% NaOH at 100 °C for 1 h	1.75	Low	Size: 50–60 mm wide, 30–200 nm long Morphology: irregular rod shape and crystal size	Selimin[191]
	Sardine (*Sardinella longiceps*)	(1) Treated with 1 N HCl (2) Treated with 1 N NaOH (3) Calcined at 600–1000 °C	n.s.[a]	High	Size: <1 μm Morphology: spherical agglomerates	Ashwitha[192]
	n.s.[a]	(1) Soaked in 40% NaOH solution (2) Ground (3) Calcined at 800 °C for 2 h	1.18	High	Size: <5 μm Morphology: irregular and uneven-sized blocks	Wang[193]
Calcination	Nile tilapia (*Oreochromis niloticus*)	(1) Calcined at 450–600 °C for 5 h (2) Collected on a 0.5-mm sieve	3.06–3.17	n.s.[a]	Size: very small	Sittitut[194]
UAE[a]	Pirarucu (*Arapaima gigas*)	(1) Calcined at 700 °C for 2 h (2) Sieved (325 mesh) (3) UAE[a] for 30 min (4) Matured for 24 h	1.58	[c]48%	Size: n.s.[a] Morphology: n.s.[a]	de Amorim[195]
	Nile tilapia (*Oreochromis niloticus*)	(1) UAE[a] with 0.8 M HCl 45 min at 60 °C (2) Added NaOH to increase pH to 12 (3) Sonicated for 30 min (4) Ground with a mortar and pestle	1.68	n.s.[a]	Size: 22.8 nm long and 8.6 nm wide Morphology: rice-shaped agglomerates	Sricharoen[196]
DES[a]	Bighead carp (*Aristichthys nobilis*)	(1) Ground and sieved (80 mesh) (2) Treated with DES[a] (choline chloride : glycerol = 1 : 2) at 70 °C for 2.5 h (3) Centrifuged for 7 min (4) Purified by stirring with 5% NaOH for 5 h at 70 °C	1.73	[c]43.1%	Size: 0.3–95 μm (median diameter 13.98 μm) Morphology: irregular and agglomerated morphology	Liu[197]
	Crucian carp (*Carassius carassius*)	(1) Ground and sieved (80 mesh) (2) Treated with DES[a] (choline chloride : 1,4-butanediol = 1 : 15) at 65 °C for 2 h (3) Centrifuged (4) Purified by stirring with 5% NaOH for 5 h at 70 °C	1.78	Low	Size: 0.235–117.1 μm (median diameter: 12.71 μm) Morphology: irregular and agglomerated morphology	Liu[198]

[a] Abbreviations – AAD, alkaline and/or acid deproteinization; UAE, ultrasound assisted extraction; DES, deep eutectic solvent; BCP, biphasic calcium phosphate; n.s., none specified. [b] Crystallinity calculated by comparing the area of crystalline peaks to the total area of amorphous and crystalline peaks (eqn (S3)). [c] Crystallinity calculated using software.

Other researchers have used AAD as a pre-treatment before calcination. Compared to fish bones that are often directly calcined without the presence of acid or base, it is much more common to deproteinize fish scales prior to thermal treatment. These methods often use dilute base rather than concentrated base because calcination will ultimately remove a significant quantity of residual protein. Like fish bones, HAP particles from scales after calcination are larger than those not exposed to high temperatures.[182,188]

3.2.3. Ultrasound assisted extraction (UAE). UAE is an extraction technique unique for fish scales that has not been extensively explored for bones yet. Note, Boudreau *et al.* have transformed fish bones to nanoparticles with UAE;[175] however this was after using solely enzymes to isolate HAP from bones.[174] UAE has been used to isolate compounds from other types of waste, specifically plant-based biomass, such as wheatgrass,[201] sugarcane bagasse,[202] coffee waste,[203] wheat straw,[204] tobacco waste,[205] and wood waste.[206] Extraction occurs when ultrasound

 © 2026 The Author(s). Published by the Royal Society of Chemistry

Open Access Article. Published on 10 ottobre 2025. Downloaded on 09/05/2026 05:18:07.
This article is licensed under a Creative Commons Attribution-NonCommercial 3.0 Unported Licence.

Table 9 Biomaterials prepared from the calcination and/or alkaline hydrolysis of fish bones/scales, published since 2019[c]

Material	Preparation	Characteristics	Reference
HAP[a] nanoparticles	(1) Alkaline hydrolysis (silver carp bones)	• Retains organic moieties to assist in better osseoinduction • Ca/P: 1.65 • Haemolytic activity 2.24[b]–3.35% at 1–5 mg mL^{-1} • 91% cell viability at 500 μL g^{-1} • Significant cell proliferation of 20% at 250 μg mL^{-1}	Acharya[216]
BCP[a] nanoparticles	(1) Calcination (silver carp bones)	• Removal of organic content and more crystalline • Ca/P: 1.45 • Haemolytic activity 3.94[b]–9.22% at 1–5 mg mL^{-1} • 86% cell viability at 500 μL g^{-1} • Cell proliferation of 15% at 250 μg mL^{-1}	Acharya[216]
HDPE[a]-BCP[a] composite	(1) Calcination (tilapia scales) (2) Spray-dried (3) 30 wt% HAP[a] mixed with HDPE[a] in extruder (4) Surface treated with MPTMS[a]	• Density: 1.17 g cm^{-3} • Melting point of 138.4 °C • Tensile strength: 28.26 MPa • Young's modulus: 1272 MPA • Elongation at break: 43.6% • Flexural strength: 21.4 MPa • Flexural modulus: 796 MPa • Impact strength: 46.90 kJ m^{-2} • 98.51% cell viability at 200 mg mL^{-1}	Aiza Jaafar[183]
BCP[a] bioceramics	(1) Calcination (salmon bones) (2) Compacted and sintered	• Density: 2.96 g cm^{-3} • Elastic modulus: 633 MPa • Ca/P: 1.67 • No cytotoxic effect compared to the control • Suitable cytocompatibility • No cell proliferation after 3 days	Bas[172]
HAP[a] particles	(1) Alkaline hydrolysis (arowana scales) (2) Calcination	• Forms a bone-like apatite layer after immersed in McCoy medium for 3 days, characterizing its bioactivity • 102.8% cell viability after 48 h	Horta[182]
BCP[a] bioceramics	(1) Calcination (tilapia bones) (2) Compacted and sintered	• Ca/P: 1.64 • Relative density: 90.92–96.43% • Vickers hardness: 5.77 GPa • Compressive stress: 89.16 MPa • Young's modulus: 13.88 GPa	Khamkongkaeo[132]
HAP[a] scaffold	(1) Calcination (tuna bones) (2) Mixed with 2% starch, compacted, and sintered	• Ca/P: 1.87 • Nontoxic behavior at concentrations <300 μg mL^{-1} • Enhanced cell proliferation over control	Mondal[131]
PLA[a]-HAP[a] filament	(1) Alkaline hydrolysis (sea bass scales) (2) Mixed with PLA[a] and eggshells (CaO) in extruder (3) Pressed into membranes	• Ca/P: 1.67 • Young's modulus: 3.52–3.95 GPa • Tensile strength: 43.1–50.9 MPa • Elongation at failure: 2.8–4.8% • Decreased water resistance • Cell viability was not different from control group at 18 days • Significantly improved cell viability compared to PLA at 2 days • Enhanced cell adhesion • Good cytocompatibility • Scavenging rate: 5–30% • Generated inhibition zones for *E. coli* and *S. aureus*	Wu[189]

Open Access Article. Published on 10 ottobre 2025. Downloaded on 09/05/2026 05:18:07. This article is licensed under a Creative Commons Attribution-NonCommercial 3.0 Unported Licence.

Table 9 (*Contd.*)

Material	Preparation	Characteristics	Reference
HAP[a] nanoparticles	(1) Alkaline hydrolysis (Indian oil sardine bones)	• Cell proliferation 141% at 100 μg mL^{-1} • Loss of contact with neighbouring cells at 250 μg mL^{-1}, suggesting higher concentrations cannot support osteoblastic growth • Good reposition of calcium in MG-63 cells at 7 days, which may be important for bone mineral density • Appropriate for cellular activities	Surya[163]
HAP[a]-CMC[a]/SA[a] coating on Ti_6Al_4V alloy	(1) Calcination (rohu bones) (2) HAP[a] added to CMC[a] in ethanol/water for 12 h (3) SA[a] added and pH adjusted to 7 (4) Ti_6Al_4V added by electrophoretic deposition	• Induces growth of apatite on composite when immersed in SBF[a] • Biomineralization evident • Microhardness value: 190 Hv • Enhanced antibacterial activity against *S. aureus* • Lower antibacterial resistance against *E. coli* • Cell viability up to 87% • No significant toxicity	Sridevi[157]
BCP[a] coating	(1) Alkaline hydrolysis (sea bream & salmon bones) (2) Calcination (3) Pressed and sintered (4) Coatings prepared by PLD[a]	• Ca/P of targets: 1.57–1.63 • Ca/P of films: 1.47–1.50 • Pull-off bonding strength sea bream: 49 MPa • Pull-off bonding strength salmon: 33 MPa • Mass gain of salmon after 7 days in DMEM[a]: 3% • Mass gain of sea bream after 7 days in DMEM[a]: 9% • Good biocompatibility • LDH[a] release salmon after 24 h: 97% of control • LDH[a] release sea bream after 24 h: 94% of control • Significantly increased anti-biofilm performances	Popescu-Pelin[142]

[a] Abbreviations – HAP, hydroxyapatite; BCP, biphasic calcium phosphates; HDPE, high-density polyethylene; MPTMS, 3-methacryloxypropyltrimethoxysilane; CMC, carboxymethylcellulose; SA, sodium alginate; SBF, simulated body fluid; PLD, pulsed laser deposition; DMEM, Dulbecco's Modified Eagle medium; LDH, lactate dehydrogenase. [b] Haemolytic activity <5% is labelled as non-haemolytic (non-toxic); haemolytic activity >5% is labelled as haemolytic (toxic). [c] Cell viability must decrease >30% to be considered cytotoxic.

(US) waves generate microbubbles containing gas and vapour within a liquid medium.[207] When the microbubbles collapse, local pressures can reach 2000 atm and temperatures increase rapidly, a phenomenon known as cavitation.[207] This process further dissolves and disintegrates solid materials into smaller particles.[207]

Compared to calcination and AAD, UAE remains relatively uncommon. In 2020, Sricharoen *et al.* applied UAE for the extraction of HAP from fish scales.[196] They performed UAE on Nile tilapia scales by immersing them in 0.2–1.2 M HCl and using ultrasonic power of 0.1–0.4 kW at 30–60 °C for 15–90 min. Based on results from ICP-AES, calcium and phosphorus extraction was optimized using 0.8 M HCl and 0.4 kW of ultrasonic power at 60 °C for 45 min. Furthermore, the pH of the solution was adjusted between 8 and 12 with NaOH, followed by sonication at 0.4 kW at room temperature for 30 min. The material was then dried, and ground with a mortar and pestle. As the pH increased, the Ca/P ratio also increased from 1.44 to 1.68 which was considered ideal since it was closest to the stoichiometric ratio of HAP. Furthermore, HAP prepared at pH 12 was the most crystalline, and rice-shaped nanoparticles (22.8 nm long and 8.6 nm in diameter) were observed while particles synthesized at lower pH had more irregular and overlapping shapes.

In the same year, Chen and co-workers also isolated HAP from Mozambique tilapia (*Oreochromis mossambicus*) scales

 © 2026 The Author(s). Published by the Royal Society of Chemistry

Open Access Article. Published on 10 ottobre 2025. Downloaded on 09/05/2026 05:18:07. This article is licensed under a Creative Commons Attribution-NonCommercial 3.0 Unported Licence.

using UAE; however they also used calcination and AAD as additional processing steps.[208] The scales were first immersed in 1 N HCl for 24 h, 1 N NaOH for 24 h, boiled at 80 °C in water for 20 min, and dried. Next, the sample was sonicated in 50% (v/v) alcohol and calcined at 1000 °C before being ground with a mortar and pestle, and passed through a 200-mesh sieve. Without calcination, the scale powder showed broad peaks in the observed XRD pattern while the calcined product matched the diffractogram of a HAP standard. The mean diameter of particles was 5.96 μm, ranging from 4.2 to 7.8 μm, values that are significantly larger than those reported by Sricharoen *et al.*[196] These values are also higher than those observed after their initial extraction technique (not incorporating UAE) where sizes ranged from 500 nm–1.5 μm.[208] This suggests that UAE might provide enough energy to grow HAP particles, similar to calcination, as similar results were observed during Boudreau *et al.*'s treatment on bones – larger particle sizes after prolonged US treatment.[175]

That being said, the opposite effect has also been observed. For example, de Amorim *et al.* also used calcination with UAE, and the heat treatment was performed before sonication.[195] Scales from pirarucu (*Arapaima gigas*) were calcined at 700 °C for 2 h and sieved through a 325-mesh sieve. While a portion of this was doped with niobium ions during UAE, some scales were not in order to see whether doping was successful. These scales were sonicated in ethanol at 20 kHz for 30 min with an amplitude of 70% and dried prior to analysis. Unlike Chen and coworkers,[208] the crystallite size decreased from 128.5 to 52.3 nm from the added UAE treatment after calcination. Furthermore, the crystallinity increased from 34 to 48%, suggesting that UAE successfully removed residual protein remaining after calcining for 2 h.

3.2.4. Deep eutectic solvents (DESs). While extraction with DESs remains the most under-researched topic discussed in this review, it is still important to mention because of its considered greenness. DESs are prepared by mixing two components that are typically solid at room temperature, but upon heating the components react to form the desired DES that remains liquid at room temperature. DESs are achieved by complexation between a hydrogen bond acceptor (HBA), typically a quaternary ammonium salt or halide salt, and a hydrogen bond donor (HBD).[209] The melting point of the mixture is lower than the melting points of individual HBA and HBD. DESs have gained significant attention among green chemists because they are typically biodegradable, nontoxic, and inexpensive with low volatility and low vapor pressure.[210] It should be highlighted, however, that not all aspects of DESs are sustainable as the HBD and/or HBA are not always green, cheap, or nontoxic.[211]

Liu *et al.* have investigated different DESs for the extraction of HAP from scales of bighead carp (*Aristichthys nobilis*)[197] in 2020 and crucian carp (*Carassius carassius*) in 2021.[198] In both cases, the scales were ground and passed through a 80 mesh sieve before being treated with DES.[197,198] For their initial study on bighead carp, three DESs were investigated – choline chloride : glycerol (1 : 2), choline chloride : citric acid (2 : 1), and choline chloride : acetic acid (1 : 2).[197] The DES that was selected as the best extraction medium was choline chloride : glycerol (1 : 2) because it had high HAP solubility, moderate viscosity, and excellent stability, and it did not decompose HAP. An optimal extraction rate of 47.67% was achieved by treating scales at 70 °C in DES for 2.5 h with a solid : liquid ratio of 1 : 15 g g^{-1}. The particles were observed to have a high median particle size of 13.98 μm and tended to agglomerate, as observed in all other methods described. Because this process does not involve high temperatures, the product was amorphous and the relative crystallinity of the extracted HAP was 43.13%. Liu *et al.* screened other DESs for HAP extraction from crucian carp scales, including choline chloride : glycerol (1 : 2), choline chloride : triethylene glycol (1 : 4), choline chloride : glycol (1 : 2), and choline chloride : 1,4-butanediol (1 : 2).[198] In this case, choline chloride : 1,4-butanediol (1 : 2) was chosen since it had the best extraction rate of 40.58%. This is interesting because this extraction rate is lower than that in their initial study where choline chloride : glycerol (1 : 2) was the best.[197] The crystallinity and median particle size diameter (12.71 μm) of crucian carp were similar to those of bighead carp.[197,198]

3.3. Applications of HAP and BCPs

3.3.1. Biomedical potential. There have been promising results using biologically sourced BCPs because of their biomimetic properties.[212] For example, incinerated fish bones have been studied for enamel remineralization and occlusion of dentin tubules.[213] Several studies have prepared HAP and/or BCPs for biomedical applications by calcining fish bones at 600–1200 °C.[172,176,214,215] One study compared the cell attachment and proliferation of two scaffolds created with synthetic HAP and tuna bones, respectively.[131] Both scaffolds were nontoxic and, despite having a Ca/P ratio of 1.87, the scaffold created with fish bones demonstrated enhanced cell proliferation and attachment. This is believed to be caused by the presence of trace elements such as Na, Mg, Sr, and Co, which better mimic human bones. Acharya *et al.* prepared nano-BCP particles from silver carp (*Hypopthalmichthys molitrix*) bones using alkaline hydrolysis and calcination separately to study the effect of extraction technique on proliferation and toxicity.[216] The particles created by alkaline hydrolysis were observed to be made of HAP and had better biocompatibility than those obtained by calcination which yielded a product containing α-TCP and β-TCP. The MG63 osteoblast cell lines had a 70.1% proliferation efficiency and 91% cell viability in cytotoxicity studies. Another variable that has been demonstrated to play a significant role in the potential of bio-derived BCPs as a bone replacement material is the species of fish from which they originate.[217] The cell proliferation and differentiation of synthetic HAP and nanoparticles from calcined rainbow trout (*Onchornuchus mkiss*), cod (*Gadus*), and salmon (*Oncorhynchus keta*) bones were studied by Shi *et al.*[217] All three samples originating from fish had superior cell viability than the synthetic, commercially sourced HAP. Salmon and rainbow trout bones significantly enhanced the viabilities which was explained by the increased substitution of CO_3^{2-} in these samples.

Open Access Article. Published on 10 ottobre 2025. Downloaded on 09/05/2026 05:18:07. This article is licensed under a Creative Commons Attribution-NonCommercial 3.0 Unported Licence.

Ultimately salmon bones were reported to be the most suitable material for bone regeneration because it stimulates cell proliferation due to its high CO_3^{2-} and Mg content.

HAP from fish bones and scales has also been shown to have enough mechanical strength for biomedical ceramics.[162] In fact, Akpan *et al.*[162] observed that BCPs from bones experienced a Vickers hardness value of 0.48 GPA which is within the range reported for human femoral cortical bone. The particles also had a fracture toughness of 5.72 MPa $m^{1/2}$ while maintaining a stable phase at 900 °C and a low brittleness index value of 0.084. Aiza Jaafar *et al.* created a high-density polyethylene (HDPE) composite incorporating BCPs obtained from the thermal degradation of fish scales at 1200 °C.[183] The size of resulting BCP particles was tailored by using spray drying and some were additionally treated with 3-methacryloxypropyltrimethoxysilane (MPTMS, $C_{10}H_{20}O_5Si$) to study its effect on the mechanical properties of composites. Young's modulus of HDPE was enhanced by 29.4% by adding 30 wt% HAP treated with MPTMS to the composite, reaching 1272 MPa, with a tensile strength of 28.26 MPa and a flexural modulus of 796 MPa. Furthermore the composite was shown by *in vitro* analyses to be non-toxic with potential to be used towards biomedical applications.

BCP materials derived from fish bones have been explored in other biomedical applications. For example, there have been several reports using BCPs from fish bones in sunscreen as an alternative to UV filters associated with health risks.[218] Adamiano *et al.* isolated BCPs from Atlantic salmon bones by calcining them at 800 °C and doped this material with Zn or Mn to increase sun protection factor (SPF)-boosting abilities.[219] Interestingly, the undoped BCP material was the most effective at increasing SPF. This demonstrates that bio-derived BCPs can be used to decrease the concentration of UV filters needed in sunscreens while maintaining high SPF values.

Table 9 lists several other example studies using BCPs sourced from fish bones and scales for biomedical purposes. Based on these reports, there is great potential for use of waste-derived HAP in bioceramics and implants, contributing towards a more sustainable industry and circular economy.

3.3.2. Environmental remediation. HAP has been studied extensively as a material for water and soil remediation because of its acid–base properties, ion-exchange capability, thermal stability, and non-toxic nature.[126] HAP's lattice is flexible and tolerant of substitutions, which explains why its carbonated version is found readily in biological systems. Cation exchange occurs through substitution of Ca^{2+} with Cu^{2+}, Mn^{2+}, Ni^{2+}, Zn^{2+}, Cd^{2+}, Co^{2+}, Mg^{2+}, Sr^{2+}, Ba^{2+}, Pb^{2+}, Al^{3+} or La^{3+}. Anion exchange can occur at OH^- and/or PO_4^{3-} sites. The OH^- has been substituted with F^-, Cl^-, Br^-, O^{2-}, and CO_3^{2-} while PO_4^{3-} has been exchanged with HPO_4^{2-}, AsO_4^{3-}, VO_4^{3-}, SO_4^{2-}, SiO_4^{4-}, and CO_3^{2-}.

Several industrial dyes have been removed from aqueous solutions using materials created with fish-derived HAP. For example, Mamum *et al.* recently prepared a photocatalyst from

Table 10 Industrial dyes treated with BCPs from fish bones/scales since 2019[a]

Preparation	Dye	Optimal conditions	Degradation/adsorption	Reference
Calcined tilapia & surma bones	Congo red	240 min,[b] 20 ppm,[c] 40 mL,[d] 0.1[e] g	65%	Mamun[148]
Pulverized silver carp bones	Congo red	240 min,[b] 200–300 ppm,[c] 100 mL,[d] 100–700 mg,[e] pH 2[f]	91–97%	Parvin[220]
Calcined shing and poa bones	Congo red	180 min,[b] 10 ppm,[c] 0.08[e] mg	73–82%	Prosad Moulick[147]
Pulverized fish bones treated with Al_2O_3	Methyl green	60 min,[b] 80 mg L^{-1},[c] 0.1 g,[e] pH 10.64,[f] 25[g] °C	92%	Al-Kazragi[222]
Calcined of catla bones	Congo red & crystal violet	75 min,[b] 50 mg L^{-1},[c] 10 mg[e]	Congo red: 87% Crystal violet: 77%	Sathiyavimal[146]
Pulverized fish bones doped with copper and calcined	Crystal violet	35 min,[b] 20 mg L^{-1},[c] 2 g L^{-1},[e] pH 10,[f] 50[g] °C	98%	Mejbar[223]
Bleached and calcined fish bones	Brilliant green	20 min,[b] 50 mg L^{-1},[c] 1 g L^{-1},[e] pH 12[f]	49.1 mg g^{-1}	Miyah[224]
Calcined fish bones	Methylene blue	10 min,[b] 100 mg L^{-1},[c] 250 mg,[e] pH 6.9,[f] 30[g] °C	>90%, 56.49 mg g^{-1}	Nurhadi[225]
Calcined catfish bones mixed with chitosan	Methylene blue & methylene orange	Methylene blue: 60 min,[b] 35 mg L^{-1},[c] 100 mL,[d] 0.1 g,[e] pH 8;[f] methylene orange: 180 min,[b] 35 mg L^{-1},[c] 100 mL,[d] 0.1 g,[e] pH 6[f]	Methylene blue: 84.89 mg g^{-1} Methylene orange: 44.05 mg g^{-1}	Trung[226]
Rohu bones treated with NaOH	Methylene blue	12 min,[b] 50 mg L^{-1},[c] pH 5;[f] 34.85[g] °C	96.1%, 666.67 mg g^{-1}	Swamiappan[227]
Rohu bones treated with NaOH	Melioderm HF brown G	120 min,[b] 200 ppm,[c] 2 g L^{-1},[e] pH 2,[f] 24.85[g] °C	98.33%	Hossain[228]

[a] Abbreviations – HAP, hydroxyapatite. [b] Reaction time for optimal dye degradation/adsorption. [c] Dye concentration for optimal dye degradation/adsorption. [d] Volume of dye solution for optimal dye degradation/adsorption. [e] Adsorbent mass/concentration for optimal dye degradation/adsorption. [f] pH for optimal dye degradation/adsorption. [g] Temperature for optimal dye degradation/adsorption.

© 2026 The Author(s). Published by the Royal Society of Chemistry

Open Access Article. Published on 10 ottobre 2025. Downloaded on 09/05/2026 05:18:07. This article is licensed under a Creative Commons Attribution-NonCommercial 3.0 Unported Licence.

Table 11 Heavy metals treated with BCPs[a] from fish bones/scales since 2020

BCP source	Additives	Metal(s)	Optimal conditions	Removal rate/adsorption	Reference
Fish bones	Chitosan, Fe_3O_4	Cd^{2+}	3 min,[b] 200 mg L^{-1},[c] 0.05 g,[d] pH 5.4,[e] 25[f] °C	25.134 mg g^{-1}	Yang[231]
Fish bones	NA[a]	Pb^{2+}	672 h,[b] 10[d] wt%	94–96%	Nag[235]
Fish scales	Polylactic acid	Pb^{2+}, Cd^{2+}	12 h,[b] 5–100 mg mL^{-1},[c] 15[d] wt%	Pb^{2+}: 112.6 mg g^{-1} Cu^{2+}: 360.5 mg g^{-1}	Fijoł[236]
Fish bones	NA[a]	Pb^{2+}, Zn^{2+}	672 h[b]	Pb^{2+}: 86.39% Zn^{2+}: 63%	Saffarzadeh[237]
Fish bones	NA[a]	Co^{2+}	400 min,[b] 10–1000 mg L^{-1},[c] 0.001 g mL^{-1}[d]	52 mg g^{-1}	Renda[144]
Fish bones	NA[a]	As^{3+}	40 min[b]	1.4 mg g^{-1}	Hubadillah[153]
Fish scales	$MgCl_2$	Cu^{2+}, Cd^{2+}, Pb^{2+}	180 min,[b] 20–800 mg L^{-1},[c] 1 mg mL^{-1},[d] pH 3–7[e]	Cu^{2+}: 84.2% Cd^{2+}: 74.2% Pb^{2+}: 53.7%	Qi[232]
Fish bones	Graphene oxide, chitosan	Cu^{2+}	120 min,[b] 100–1000 mg L^{-1},[c] 1 mg mL^{-1},[d] pH 5[e]	256.41 mg g^{-1}	Hoa[238]

[a] Abbreviations – BCP, biphasic calcium phosphate; HAP, hydroxyapatite; NA, not applicable. [b] Reaction time. [c] Heavy metal concentration. [d] Adsorbent mass/concentration. [e] pH for optimal dye degradation/adsorption. [f] Temperature for optimal degradation/adsorption.

calcined tilapia and surma bones for the degradation of Congo red dye,[148] an environmental pollutant. In a similar study, pama croaker and Asian stinging catfish were used to create the same photocatalyst, achieving degradation rates of 82% and 73%, respectively, towards Congo red.[147] That being said, much higher degradation rates of up to 97% were reported by Biswas and co-workers using raw, pulverized silver carp bones.[220] This is interesting because the product contains significantly higher quantities of organic impurities compared to other photocatalysts due to the lack of heat or alkaline treatment. Congo red has anionic sites from sulfonate groups, and other anionic dyes have been studied (*e.g.*, acid blue 185),[221] while neutral and cationic dyes have also been successfully treated with fish bones such as methyl green,[222] crystal violet,[146,223] brilliant green,[224] and methylene blue.[225] (Table 10).

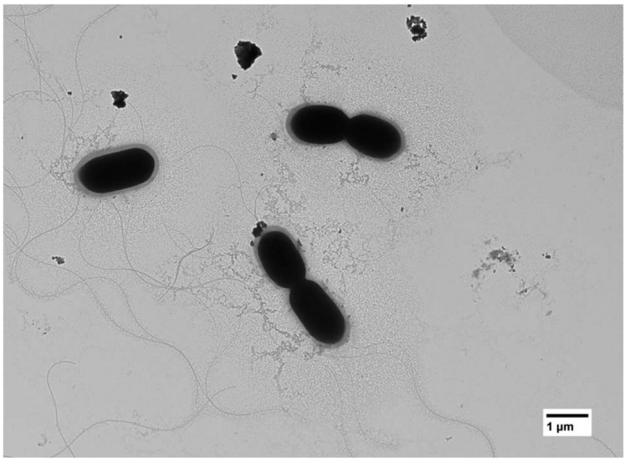

Fig. 6 TEM image obtained when HAP nanoparticles prepared in water were allowed to sit at room temperature for several days (SI). The black cylindrical particles approximately 1 µm in diameter are attributed to unspecified bacteria.

Other pollutants besides dyes have been treated with HAP derived from fish discards. Synthetic HAP has been studied widely for the removal of a broad range of of heavy metals.[229,230] There have been several studies using bio-sourced HAP to remediate Cd^{2+},[231,232] Pb^{2+},[232–237] Co^{2+},[144] As^{3+},[153] Zn^{2+},[237] and Cu^{2+}[232,238] (Table 11). For example, Cd^{2+} and Pb^{2+} have been successfully adsorbed from water by Rashed *et al.* using calcined fish bones.[239] A 99% removal rate of Cd^{2+} and Pb^{2+} was achieved by treating wastewater with 0.1 g HAP for 30 min at ~55 °C with a metal concentration of 10 ppm.[239] Renda *et al.* discovered that HAP could also be used for the adsorption and desorption of Co^{2+} ions from aqueous solutions.[144] Co^{2+} is a controversial heavy metal because of its effect on human health, but it is also necessary in small quantities for certain bodily functions (*e.g.*, vitamin B_{12}, essential coenzyme for cell mitosis, metabolism, and N_2 fixation) and industrial applications (*e.g.*, mining, electronics, and electroplating). The desorbed Co^{2+} was then observed to have beneficial effects towards seed germination and root elongation.

4. Conclusions

There has been a significant increase in fish production over the last few decades to meet the demands of a growing human population. This has led to an abundance of seafood processing byproducts being disposed of unsustainably, contributing to greenhouse gas emissions, eutrophication, and ocean acidification. There have been several global examples that demonstrate that it is possible to process each portion of fish to higher value products instead of just focusing on the edible portion as being of sole value. Iceland's 100% Fish Project has created many different products from fish including fish leather. Norway has also been making great progress towards whole fish utilization. However, these examples face regulatory challenges.[22–24] While successes have been achieved with new products based on marine collagen and materials from fish

Open Access Article. Published on 10 ottobre 2025. Downloaded on 09/05/2026 05:18:07. This article is licensed under a Creative Commons Attribution-NonCommercial 3.0 Unported Licence.

skin, there are, as far as we are aware, no commercial processes focused on the inorganic components present in seafood waste.

In this review, we have summarized the possibilities of isolating valuable biominerals from fish inedible discards. In general, it is more advantageous to source calcium-based materials naturally instead of producing them synthetically for sustainability and applicability purposes. Valorizing by-products from the seafood processing industry offers additional streams for financial gain, and prevents significant food waste from ending up in landfills and/or the ocean. This would limit GHG emissions, eutrophication, groundwater contaminations, and odor nuisances caused by the wasted discards. Specifically, this topic tackles many of the UN SDGs, including UN SDG2: Zero Hunger, UN SDG3: Good Health & Well-Being, UN SDG8: Decent Work and Economic Growth, UN SDG9: Industry, Innovation and Infrastructure, UN SDG11: Sustainable Cities and Communities, UN SDG12: Responsible Consumption and Production, UN SDG13: Climate Action, and UN SDG14: Life Below Water. While synthetic $CaCO_3$ and HAP continue to be used more prominently than biogenic materials for most applications, the biomimetic properties of natural HAP and $CaCO_3$ could make it more advantageous for biomedical purposes (*e.g.*, enhanced biomineralization).

Shells from bivalves, crustaceans, and gastropods have the potential to be used as a feedstock for $CaCO_3$ which can then be converted to other value-added products, including CaO and PCC. An interesting area of research that could be investigated is the tailored morphology of polymorphs. While specific polymorphs have been achieved through PCC processes, calcite itself has a range of morphologies that could be explored for biomedical purposes. Khanjani *et al.* recently explored the factors that influence the morphology of microbially induced PCC, discovering that Ca^{2+} and functional groups present have an impact on the resulting polymorph and shape.[240] While this study primarily focused on vaterite and calcite's spherical shape, it would be interesting to study other possible morphologies.

HAP has been isolated from fish bones and scales using a range of techniques including calcination, alkaline/acidic deproteinization, enzymatic hydrolysis, ultrasound assisted extraction, and the use of deep eutectic solvents. This bio-derived HAP product has been explored for various applications such as incorporation into biomedical composites and the treatment of heavy metals and industrial dyes. These processes have the potential to mitigate the large number of byproducts wasted in landfills and the ocean, although there are some drawbacks. While some reports have focused specifically on making their treatment sustainable and scalable (*e.g.*, enzymes), many of the processes described are industrially inapplicable in seafood processing plants, requiring high temperatures for calcination and the use of hazardous chemicals such as concentrated base (*e.g.*, KOH 50 wt%) for deproteinization. There are also inconsistencies in particle size and morphology of products originating from the same species of fish. One of the main drawbacks of studying biomass-derived products is the development of bacteria, especially in samples that contain trace amounts of residual protein. In fact, we have observed bacteria in TEM images of some of our own HAP nanoparticle solutions from fish bone that were left at room temperature (Fig. 6). For future studies, it would be interesting to develop a low temperature method without the use of acids or bases that also prevents the growth of potentially harmful bacteria. This would ensure that $CaCO_3$ and HAP can be produced sustainably from seafood discards while also being suitable for biomedical purposes. Reduction in endotoxin contamination has been important in advancing the use of organic products such as chitosan from seafood waste streams.[241] As the global seafood industry continues to shift from wild catch to aquaculture practices, several threats have emerged. Some of these include the spread of diseases between wild fish and farmed fish and the risk of rising ocean temperatures from climate change affecting harvested species. By completely valorizing every aspect of caught marine organisms, industries would be able to continue making a profit despite challenges with the edible portion. Therefore, the fish itself would remain useful and valuable even if not being considered seafood. For food production, it is important to adapt to climate change and consider indoor recirculating aquaculture systems instead of open ocean systems to mitigate the variations in water temperature and composition.

Author contributions

Conceptualization, F. M. K. and S. B.; writing – original draft preparation, S. B.; writing – review and editing, S. B., E. L., and F. M. K.; supervision, E. L. and F. M. K.; funding acquisition, E. L. and F. M. K.

Conflicts of interest

There are no conflicts to declare.

Data availability

There is limited supporting data for this review article. The instrumental conditions for Fig. 6 are described in Boudreau *et al.*'s article in *RSC Sustainability* (2025) and in the supplementary information file (SI) for this review. Supplementary information is available. See DOI: **https://doi.org/10.1039/d5su00527b**.

Acknowledgements

We thank the NRC Ocean program, OGEN (OCN-110-4), OFI, NSERC of Canada, Memorial University of Newfoundland (MUN), and Dr Liqin Chen for funding.

References

1 A. Estim, R. Shapawi, S. R. M. Shaleh, C. Fui-Fui and S. Mustafa, in *SDGs in the Asia and Pacific Region*, Springer, Cham, 2024, pp. 415–444.
2 J. R. Stevens, R. W. Newton, M. Tlusty and D. C. Little, *Mar. Pol.*, 2018, **90**, 115–124.

© 2026 The Author(s). Published by the Royal Society of Chemistry

Open Access Article. Published on 10 ottobre 2025. Downloaded on 09/05/2026 05:18:07. This article is licensed under a Creative Commons Attribution-NonCommercial 3.0 Unported Licence.

3 Fish and seafood consumption per capita, 2020, https://ourworldindata.org/grapher/fish-and-seafood-consumption-per-capita?tab=table&time=earliest, accessed August 14, 2025.
4 Fish and overfishing, https://ourworldindata.org/fish-and-overfishing, accessed August 14, 2025.
5 Capture fisheries production, https://www.fao.org/3/cc0461en/online/sofia/2022/capture-fisheries-production.html, accessed August 14, 2025.
6 S. Idowu, R. Schmidpeter, N. Capaldi, L. Zu, M. D. Baldo and R. Abreu, *Encyclopedia of Sustainable Management*, Springer Nature, 2023.
7 FAO leads global efforts to strengthen aquaculture for food and sustainable development, https://www.fao.org/newsroom/detail/fao-leads-global-efforts-to-strengthen-aquaculture-for-food-and-sustainable-development/en, accessed August 14, 2025.
8 Aquaculture – Fisheries and Aquaculture, https://www.fao.org/fishery/en/topic/16064, accessed August 14, 2025.
9 Aquaculture production, https://www.fao.org/3/cc0461en/online/sofia/2022/aquaculture-production.html, accessed August 14, 2025.
10 K. Greer, D. Zeller, J. Woroniak, A. Coulter, M. Winchester, M. L. D. Palomares and D. Pauly, *Mar. Policy*, 2019, **107**, 103382.
11 E. Gilman, M. Musyl, P. Suuronen, M. Chaloupka, S. Gorgin, J. Wilson and B. Kuczenski, *Sci. Rep.*, 2021, **11**, 7195.
12 Aquaculture|Food Loss and Waste in Fish Value Chains|Food and Agriculture Organization of the United Nations, https://www.fao.org/flw-in-fish-value-chains/value-chain/aquaculture/en/, accessed August 14, 2025.
13 Processing & Storage|Food Loss and Waste in Fish Value Chains|Food and Agriculture Organization of the United Nations, https://www.fao.org/flw-in-fish-value-chains/value-chain/processing-storage/en/, accessed August 14, 2025.
14 K. Mazik, D. Burdon and M. Elliott, *Seafood-waste Disposal at Sea – a Scientific review., Institute of Estuarine & Coastal Studies*, University of Hull, Hull, UK, 2005.
15 Tackling food loss and waste, https://www.fao.org/newsroom/detail/FAO-UNEP-agriculture-environment-food-loss-waste-day-2022/en, accessed August 14, 2025.
16 J. W. Levis and M. A. Barlaz, *Environ. Sci. Technol.*, 2011, **45**, 7438–7444.
17 A. A. Ansari and S. S. Gill, *Eutrophication: Causes, Consequences and Control: Volume 2*, Springer Science & Business Media, 2013.
18 M. F. Chislock, E. Doster, R. A. Zitomer and A. E. Wilson, *Nat. Educ. Knowl.*, 2013, **4**, 10.
19 Eutrophication, https://www.nature.com/scitable/knowledge/library/eutrophication-causes-consequences-and-controls-in-aquatic-102364466/, accessed August 14, 2025.
20 N. O. and A. A. US Department of Commerce, What is eutrophication?, https://oceanservice.noaa.gov/facts/eutrophication.html, accessed August 14, 2025.
21 Z. Fadeeva and R. Van Berkel, in *Sustainable Food Value Chain Development*, Springer, Singapore, 2023, pp. 61–86.
22 A. V. Strand, S. Mehta, M. S. Myhre, G. Ólafsdóttir and N. M. Saviolidis, *Resour. Environ. Sustain.*, 2024, **16**, 100157.
23 100% Fish, https://sjavarklasinn.is/en/iceland-ocean-cluster/100-fish/, accessed August 14, 2025.
24 D. C. Finger, G. Saevarsdottir, H. G. Svavarsson, B. Björnsdóttir, S. Arason and L. Böhme, *Circ. Econ. Sustain.*, 2021, **1**, 525–543.
25 D. Coppola, M. Oliviero, G. A. Vitale, C. Lauritano, I. D'Ambra, S. Iannace and D. de Pascale, *Mar. Drugs*, 2020, **18**, 214.
26 D. Dave, V. vasudevan ramakrishnan, J. Pohling, S. Cheema, S. Trenholm, H. Burke and W. Murphy, *J. Food Process. Technol.*, 2014, **5**, 1000401.
27 R. Melgosa, M. T. Sanz and S. Beltrán, *J. Supercrit. Fluids*, 2021, **169**, 105121.
28 C. M. Laprise, K. A. Hawboldt, F. M. Kerton and C. M. Kozak, *Macromol. Rapid Commun.*, 2021, **42**, 2000339.
29 E. Paone, F. Fazzino, D. M. Pizzone, A. Scurria, M. Pagliaro, R. Ciriminna and P. S. Calabrò, *Sustainability*, 2021, **13**, 2428.
30 N. Yan and X. Chen, *Nature*, 2015, **524**, 155–157.
31 T. Jin, T. Liu, E. Lam and A. Moores, *Nanoscale Horiz.*, 2021, **6**, 505–542.
32 J. L. Vidal, T. Jin, E. Lam, F. Kerton and A. Moores, *Curr. Res. Green Sustainable Chem.*, 2022, **5**, 100330.
33 H. J. Burke and F. Kerton, *Mar. Drugs*, 2023, **21**, 366.
34 J. L. Shamshina and P. Berton, *Front. Bioeng. Biotechnol.*, 2020, **8**, 00011.
35 M. Khajavian, V. Vatanpour, R. Castro-Muñoz and G. Boczkaj, *Carbohydr. Polym.*, 2022, **275**, 118702.
36 P. A. Aneesh, R. Anandan, L. R. G. Kumar, K. K. Ajeeshkumar, K. A. Kumar and S. Mathew, *Biomass Convers. Biorefinery*, 2023, **13**, 205–214.
37 F. Hajiali, J. Vidal, T. Jin, L. C. de la Garza, M. Santos, G. Yang and A. Moores, *ACS Sustainable Chem. Eng.*, 2022, **10**, 11348–11357.
38 Mining facts – Teaching activities, https://www.dnr.state.mn.us/education/teachers/activities/soudan_mine/miningfacts.html, accessed August 14, 2025.
39 W. H. Langer, in *Encyclopedia of Materials: Science and Technology*, ed. K. H. J. Buschow, R. W. Cahn, M. C. Flemings, B. Ilschner, E. J. Kramer, S. Mahajan and P. Veyssière, Elsevier, Oxford, 2001, pp. 1537–1545.
40 *Calcium Carbonate: from the Cretaceous Period into the 21st Century*, ed. F. W. Tegethoff, J. Rohleder and E. Kroker, Birkhäuser Verlag, Basel; Boston, English edn, 2001.
41 D. Cree and A. Rutter, *ACS Sustainable Chem. Eng.*, 2015, **3**, 941–949.
42 A. Dowling, J. O'Dwyer and C. C. Adley, *J. Clean. Prod.*, 2015, **92**, 13–22.
43 U. S. G. Survey, *Mineral Commodity Summaries 2024*, U.S. Geological Survey, 2024.

Open Access Article. Published on 10 ottobre 2025. Downloaded on 09/05/2026 05:18:07. This article is licensed under a Creative Commons Attribution-NonCommercial 3.0 Unported Licence.

44 O. US EPA, *AP 42*, 5th edn, ch. 11, vol. 1, https://www.epa.gov/air-emissions-factors-and-quantification/ap-42-fifth-edition-volume-i-chapter-11-mineral-products-0, accessed August 14, 2025.
45 J. M. Paris, J. G. Roessler, C. C. Ferraro, H. D. DeFord and T. G. Townsend, *J. Clean. Prod.*, 2016, **121**, 1–18.
46 K. M. Ripley, F. H. Saadi and Z. L. Burke, *RSC Sustain.*, 2025, **3**, 255–263.
47 M. Simoni, M. D. Wilkes, S. Brown, J. L. Provis, H. Kinoshita and T. Hanein, *Renew. Sustain. Energy Rev.*, 2022, **168**, 112765.
48 C. Rodriguez-Navarro, E. Ruiz-Agudo, A. Luque, A. B. Rodriguez-Navarro and M. Ortega- Huertas, *Am. Mineral.*, 2009, **94**, 578–593.
49 O. A. Jimoh, A. K. Shah, H. B. Hussin and A. E. Temitope, *Carbonates Evaporites*, 2018, **33**, 331–346.
50 International Energy Agency, *Technology Roadmap – Low-Carbon Transition in the Cement Industry*, 2018.
51 J. Rissman, C. Bataille, E. Masanet, N. Aden, W. R. Morrow, N. Zhou, N. Elliott, R. Dell, N. Heeren, B. Huckestein, J. Cresko, S. A. Miller, J. Roy, P. Fennell, B. Cremmins, T. Koch Blank, D. Hone, E. D. Williams, S. de la Rue du Can, B. Sisson, M. Williams, J. Katzenberger, D. Burtraw, G. Sethi, H. Ping, D. Danielson, H. Lu, T. Lorber, J. Dinkel and J. Helseth, *Appl. Energy*, 2020, **266**, 114848.
52 S. Kittipongvises, *Environ. Clim. Technol.*, 2017, **20**, 67–83.
53 G. M. Naja, R. Rivero, S. E. Davis and T. Van Lent, *Water, Air, Soil Pollut.*, 2011, **217**, 95–104.
54 Y. I. Stepkin, T. I. Prozhorina, S. A. Kurolap, O. V. Klepikov and A. S. Boeva, *J. Phys.: Conf. Ser.*, 2021, **1889**, 032028.
55 Y.-Q. Niu, J.-H. Liu, C. Aymonier, S. Fermani, D. Kralj, G. Falini and C.-H. Zhou, *Chem. Soc. Rev.*, 2022, **51**, 7883–7943.
56 M. H. Azarian and W. Sutapun, *Front. Mater.*, 2022, **9**, 1024977.
57 J. A. H. Oates, *Lime and Limestone: Chemistry and Technology, Production and Uses*, John Wiley & Sons, 2008.
58 F. M. Kerton, *RSC Sustain.*, 2023, **1**, 401–403.
59 N. Vieira Veríssimo, C. Ussemane Mussagy, A. Alves Oshiro, C. M. Nóbrega Mendonça, V. de Carvalho Santos-Ebinuma, A. Pessoa, R. P. de Souza Oliveira and J. F. Brandão Pereira, *Green Chem.*, 2021, **23**, 9377–9400.
60 F. M. Kerton, Y. Liu, K. W. Omari and K. Hawboldt, *Green Chem.*, 2013, **15**, 860–871.
61 M. A. Yusoff, P. Mohammadi, F. Ahmad, N. A. Sanusi, H. Hosseinzadeh-Bandbafha, H. Vatanparast, M. Aghbashlo and M. Tabatabaei, *Sci. Total Environ.*, 2024, **952**, 175810.
62 A. Singh, N. Kelkar, K. Natarajan and S. Selvaraj, *Environ. Sci. Pollut. Res.*, 2021, **28**, 46985–46998.
63 F. Soost, *Chirurg*, 1996, **67**, 1193–1196.
64 M. Ni and B. D. Ratner, *Surf. Interface Anal.*, 2008, **40**, 1356–1361.
65 R. A. Boulos, F. Zhang, E. S. Tjandra, A. D. Martin, D. Spagnoli and C. L. Raston, *Sci. Rep.*, 2014, **4**, 3616.
66 R. Febrida, S. Setianto, E. Herda, A. Cahyanto and I. M. Joni, *Heliyon*, 2021, **7**, e08344.
67 W. L. Bragg, *Proc. R. Soc. London, Ser. A*, 1997, **105**, 16–39.
68 J. N. Murphy, C. M. Schneider, L. K. Mailänder, Q. Lepillet, K. Hawboldt and F. M. Kerton, *Green Chem.*, 2019, **21**, 3920–3929.
69 A. G. Christy, *Cryst. Growth Des.*, 2017, **17**, 3567–3578.
70 F. Liendo, M. Arduino, F. A. Deorsola and S. Bensaid, *Powder Technol.*, 2022, **398**, 117050.
71 A. Prihanto, S. Muryanto, R. Ismail, J. Jamari and A. P. Bayuseno, *Environ. Technol.*, 2024, **45**, 235–245.
72 R. Ismail, D. F. Fitriyana, Y. I. Santosa, S. Nugroho, A. J. Hakim, M. S. Al Mulqi, J. Jamari and A. P. Bayuseno, *J. Cryst. Growth*, 2021, **572**, 126282.
73 A. P. Bayuseno, A. I. Prasetya, R. Ismail, B. Setiyana and J. Jamari, *Rasayan J. Chem.*, 2022, **15**, 523–528.
74 F. M. Kerton and N. Yan, *Fuels, Chemicals and Materials from the Oceans and Aquatic Sources*, John Wiley & Sons, 2017.
75 J.-A. Barrat, L. Chauvaud, F. Olivier, P. Poitevin and M.-L. Rouget, *Chem. Geol.*, 2023, **638**, 121695.
76 J. N. Murphy, K. Hawboldt and F. M. Kerton, *Green Chem.*, 2018, **20**, 2913–2920.
77 C. Triunfo, S. Gärtner, C. Marchini, S. Fermani, G. Maoloni, S. Goffredo, J. G. Morales, H. Cölfen and G. Falini, *ACS Omega*, 2022, **7**, 43992–43999.
78 C. C. Cardoso, A. S. Cavalcanti, R. O. Silva, S. Alves Junior, F. P. de Sousa, V. M. D. Pasa, S. Arias and J. G. A. Pacheco, *J. Braz. Chem. Soc.*, 2020, **31**, 756–767.
79 J. N. Murphy, C. M. Schneider, K. Hawboldt and F. M. Kerton, *Matter*, 2020, **3**, 2029–2041.
80 M. F. R. S. Araújo, P. C. Lima, C. C. Cardoso and V. M. D. Pasa, *J. Clean. Prod.*, 2020, **277**, 123709.
81 K.-W. Nam, S.-W. Lee, J.-H. Song, H.-D. Jeung and K.-I. Park, *Korean J. Malacol.*, 2015, **31**, 279–283.
82 K. Anand, M. Reshma, M. Kannan, M. Selvan, S. Chaturvedi, A. Shalan and K. Govindaraju, *J. Nanostruct. Chem.*, 2021, **11**, 409–422.
83 E. Águila-Almanza, H. Hernández-Cocoletzi, E. Rubio-Rosas, M. Calleja-González, H. R. Lim, K. S. Khoo, V. Singh, J. C. Maldonado-Montiel and P. L. Show, *Chemosphere*, 2022, **288**, 132550.
84 C. Ramakrishna, T. Thenepalli, C. Han and J.-W. Ahn, *Korean J. Chem. Eng.*, 2017, **34**, 225–230.
85 B. Nguyen Quang and D. Ta Hong, *J. Chem.*, 2022, **2022**, e3821717.
86 L. Ogresta, F. Nekvapil, T. Tămaş, L. Barbu-Tudoran, M. Suciu, R. Hirian, M. Aluaş, G. Lazar, E. Levei, B. Glamuzina and S. C. Pinzaru, *ACS Omega*, 2021, **6**, 27773–27780.
87 R. Ismail, T. Cionita, W. L. Shing, D. F. Fitriyana, J. P. Siregar, A. P. Bayuseno, F. W. Nugraha, R. C. Muhamadin, R. Junid and N. A. Endot, *Materials*, 2022, **15**, 5712.
88 K. H. Mo, U. J. Alengaram, M. Z. Jumaat, S. C. Lee, W. I. Goh and C. W. Yuen, *Constr. Build. Mater.*, 2018, **162**, 751–764.
89 E.-I. Yang, S.-T. Yi and Y.-M. Leem, *Cem. Concr. Res.*, 2005, **35**, 2175–2182.
90 S.-H. Eo and S.-T. Yi, *Mag. Concr. Res.*, 2015, **67**, 833–842.

© 2026 The Author(s). Published by the Royal Society of Chemistry

Open Access Article. Published on 10 ottobre 2025. Downloaded on 09/05/2026 05:18:07. This article is licensed under a Creative Commons Attribution-NonCommercial 3.0 Unported Licence.

91 C. Varhen, S. Carrillo and G. Ruiz, *Constr. Build. Mater.*, 2017, **136**, 533–540.
92 H. Cuadrado-Rica, N. Sebaibi, M. Boutouil and B. Boudart, *Mater. Struct.*, 2016, **49**, 1805–1816.
93 N. H. Othman, B. H. A. Bakar, M. M. Don and M. A. M. Johari, *J. Civ. Eng.*, 2013, **25**, 201–211.
94 K. Muthusamy, S. M. A. Nasir and A. M. Budiea, *Concr. Res. Lett.*, 2016, **7**, 132–137.
95 P. Lertwattanaruk, N. Makul and C. Siripattarapravat, *J. Environ. Manag.*, 2012, **111**, 133–141.
96 S. Christian-Robinson and F. M. Kerton, *Pure Appl. Chem.*, 2024, **96**, 1247–1255.
97 J. N. Murphy, M. A. Morgan, S. Christian-Robinson, M. M. Fitzgerald and F. M. Kerton, *Can. J. Chem.*, 2025, 1–10.
98 M. M. Fitzgerald, M. A. Morgan and F. M. Kerton, *J. Sustain. Circ. NOW*, 2025, **02**, a24874285.
99 K. M. Ibiyeye and A. B. Z. Zuki, *Int. J. Mol. Sci.*, 2020, **21**, 1900.
100 K. M. Ibiyeye, A. B. Z. Zuki, N. Nurdin and M. Ajat, *Nanosci. Nanotechnol.–Asia*, 2020, **10**, 518–533.
101 S. Dampang, E. Purwanti, F. Destyorini, S. B. K. B. Kurniawan, S. R. S. Abdullah and M. F. Imron, *J. Econ. Eng.*, 2021, **22**, 221–228.
102 N. F. Nasir and M. M. Hazri, *Res. Prog. Mech. Manuf. Eng.*, 2020, **1**, 44–55.
103 M. V. S. Rezende, U. C. Pereira, Y. R. R. S. Rezende, I. S. Carvalho, W. S. Silveira, D. O. Junot, R. S. Silva, C. X. Resende and N. S. Ferreira, *Optik*, 2021, **235**, 166636.
104 Y. Wibisono, S. R. Ummah, M. B. Hermanto, G. Djoyowasito and A. Noviyanto, *Res. Eng.*, 2024, **21**, 101781.
105 J. H. Seo, S. M. Park, B. J. Yang and J. G. Jang, *Materials*, 2019, **12**, 1322.
106 W. Kurdowski, in *Cement and Concrete Chemistry*, Springer, Dordrecht, 2014, pp. 21–127.
107 A. Hart, *Waste Manag. Res.*, 2020, **38**, 514–527.
108 S. Thakur, S. Singh and B. Pal, *Fuel Process. Technol.*, 2021, **213**, 106707.
109 S. Gohar Khan, M. Hassan, M. Anwar, Zeshan, U. Masood Khan and C. Zhao, *Fuel*, 2022, **330**, 125480.
110 N. O. Eddy, A. O. Odiongenyi, R. Garg, R. A. Ukpe, R. Garg, A. E. Nemr, C. M. Ngwu and I. J. Okop, *Environ. Sci. Pollut. Res.*, 2023, **30**, 64036–64057.
111 E. C. Ogoko, H. I. Kelle, O. Akintola and N. O. Eddy, *Biomass Convers. Biorefinery*, 2024, **14**, 14859–14875.
112 N. Erdogan and H. A. Eken, *Physicochem. Probl. Miner. Process.*, 2017, **53**, 57–68.
113 Precipitated Calcium Carbonate, **https://www.lime.org/resource/other-uses-of-lime/**, accessed August 14, 2025.
114 M. Eriksson, K. Sandström, M. Carlborg and M. Broström, *Minerals*, 2024, **14**, 244.
115 M. A. Irfa'i, A. Prihanto, S. Muryanto, J. Jamari, R. Ismail and A. P. Bayuseno, *IOP Conf. Ser. Earth Environ. Sci.*, 2022, **1098**, 012021.
116 X. Feng, *Curr. Chem. Biol.*, 2009, **3**, 189–196.
117 R.-M. Kavasi, C. C. Coelho, V. Platania, P. A. Quadros and M. Chatzinikolaidou, *Nanomaterials*, 2021, **11**, 1152.
118 P. Dan, V. Sundararajan, H. Ganeshkumar, B. Gnanabarathi, A. K. Subramanian, G. D. Venkatasubu, S. Ichihara, G. Ichihara and S. Sheik Mohideen, *Appl. Surf. Sci.*, 2019, **484**, 568–577.
119 K. Kuroda and M. Okido, *Bioinorgan. Chem. Appl.*, 2012, **2012**, 730693.
120 S.-M. Huang, S.-M. Liu, C.-L. Ko and W.-C. Chen, *Polymers*, 2022, **14**, 976.
121 S. Awasthi, S. Kumar Pandey, E. Arunan and C. Srivastava, *J. Mater. Chem. B*, 2021, **9**, 228–249.
122 Y. Yang, J. Yang, N. Zhu, H. Qiu, W. Feng, Y. Chen, X. Chen, Y. Chen, W. Zheng, M. Liang, T. Lin, J. Yu and Z. Guo, *J. Nanobiotechnol.*, 2023, **21**, 470.
123 M. Du, J. Chen, K. Liu, H. Xing and C. Song, *Compos. B Eng.*, 2021, **215**, 108790.
124 S. Balhuc, R. Campian, A. Labunet, M. Negucioiu, S. Buduru and A. Kui, *Crystals*, 2021, **11**, 674.
125 T. U. Habibah, D. V. Amlani and M. Brizuela, in *StatPearls*, StatPearls Publishing, Treasure Island (FL), 2024.
126 M. Ibrahim, M. Labaki, J.-M. Giraudon and J.-F. Lamonier, *J. Hazard. Mater.*, 2020, **383**, 121139.
127 A. Fihri, C. Len, R. S. Varma and A. Solhy, *Coord. Chem. Rev.*, 2017, **347**, 48–76.
128 A. Das and D. Pamu, *Mater. Sci. Eng., C*, 2019, **101**, 539–563.
129 N. A. S. Mohd Pu'ad, R. H. Abdul Haq, H. Mohd Noh, H. Z. Abdullah, M. I. Idris and T. C. Lee, *Mater. Today Proc.*, 2020, **29**, 233–239.
130 J. M. Delgado-López and M. Iafisco, *Apatite: Synthesis, Structural Characterization, and Biomedical Applications*, Nova Science Publishers, Inc, New York, 2014.
131 S. Mondal, G. Hoang, P. Manivasagan, M. S. Moorthy, H. H. Kim, T. T. Vy Phan and J. Oh, *Mater. Chem. Phys.*, 2019, **228**, 344–356.
132 A. Khamkongkaeo, T. Boonchuduang, W. Klysubun, P. Amonpattaratkit, H. Chunate, N. Tuchinda, A. Pimsawat, S. Daengsakul, P. Suksangrat, W. Sailuam, D. Vongpramate, A. Bootchanont and B. Lohwongwatana, *Ceram. Int.*, 2021, **47**, 34575–34584.
133 K. A. Zakaria, N. I. Yatim, N. Ali and H. Rastegari, *Environ. Sci. Pollut. Res.*, 2022, **29**, 46471–46486.
134 M. Greiner, L. Férnandez-Díaz, E. Griesshaber, M. N. Zenkert, X. Yin, A. Ziegler, S. Veintemillas-Verdaguer and W. W. Schmahl, *Minerals*, 2018, **8**, 315.
135 J. A. Ruben and A. A. Bennett, *Evolution*, 1987, **41**, 1187–1197.
136 A. Maidaniuc, F. Miculescu, R. C. Ciocoiu, T. M. Butte, I. Pasuk, G. E. Stan, S. I. Voicu and L. T. Ciocan, *Ceram. Int.*, 2020, **46**, 10159–10171.
137 M. R. Hasan, N. S. M. Yasin, M. S. M. Ghazali and N. F. Mohtar, *J. Sustain. Sci. Manag.*, 2020, **15**, 9–21.
138 M. R. Hasan, M. S. M. Ghazali and N. F. Mohtar, *J. Mech. Eng. Sci.*, 2021, **15**, 7792–7806.
139 P. Ideia, L. Degli Esposti, C. C. Miguel, A. Adamiano, M. Iafisco and P. C. Castilho, *Int. J. Appl. Ceram. Technol.*, 2021, **18**, 235–243.

Open Access Article. Published on 10 ottobre 2025. Downloaded on 09/05/2026 05:18:07. This article is licensed under a Creative Commons Attribution-NonCommercial 3.0 Unported Licence.

140 H. A. Permatasari, R. Wati, R. M. Anggraini, A. Almukarramah and Y. Yusuf, *Key Eng. Mater.*, 2020, **840**, 318–323.
141 F. Fendi, B. Abdullah, S. Suryani, I. Raya and D. Tahir, *IOP Conf. Ser. Earth Environ. Sci.*, 2023, **1230**, 012042.
142 G. Popescu-Pelin, C. Ristoscu, L. Duta, I. Pasuk, G. E. Stan, M. S. Stan, M. Popa, M. C. Chifiriuc, C. Hapenciuc, F. N. Oktar, A. Nicarel and I. N. Mihailescu, *Mar. Drugs*, 2020, **18**, 623.
143 S. Lestari, M. Nurhadi, R. K. Wardani, E. Saputro, R. Pujisupiati, N. S. Muskita, N. Fortuna, A. S. Purwandari, F. Aryani, S. Y. Lai and H. Nur, *Bull. Chem. React. Eng. Catal.*, 2022, **17**, 565–576.
144 C. G. Renda, T. M. D. O. Ruellas, J. O. D. Malafatti, C. S. S. Araújo, G. L. da Silva, B. A. M. Figueira, S. Quaranta and E. C. Paris, *Physchem*, 2023, **3**, 34–60.
145 A. Q. Ishak, N. A. N. Ali, A. M. S. Nurhaziqah and H. Salleh, *Solid State Phenom.*, 2020, **307**, 339–344.
146 S. Sathiyavimal, S. Vasantharaj, M. Shanmugavel, E. Manikandan, P. Nguyen-Tri, K. Brindhadevi and A. Pugazhendhi, *Prog. Org. Coating*, 2020, **148**, 105890.
147 S. Prosad Moulick, Md. Sahadat Hossain, Md. Zia Uddin Al Mamun, F. Jahan, Md. Farid Ahmed, R. A. Sathee, Md. Sujan Hossen, Md. Ashraful Alam, Md. Sha Alam and F. Islam, *Results Eng.*, 2023, **20**, 101418.
148 M. Z. U. A. Mamun, M. S. Hossain, S. P. Moulick, M. Begum, R. A. Sathee, M. S. Hossen, F. Jahan, M. M. Rashid, F. Islam, R. H. Bhuiyan and M. S. Alam, *Heliyon*, 2023, **9**, e18012.
149 A. Pal, S. Paul, A. R. Choudhury, V. K. Balla, M. Das and A. Sinha, *Mater. Lett.*, 2017, **203**, 89–92.
150 H. B. Modolon, J. Inocente, A. M. Bernardin, O. R. Klegues Montedo and S. Arcaro, *Ceram. Int.*, 2021, **47**, 27685–27693.
151 P. Satish, A. Salian, K. Hadagalli and S. Mandal, *Adv. Appl. Ceram.*, 2023, **122**, 69–78.
152 F. Carella, M. Seck, L. D. Esposti, H. Diadiou, A. Maienza, S. Baronti, P. Vignaroli, F. P. Vaccari, M. Iafisco and A. Adamiano, *J. Environ. Chem. Eng.*, 2021, **9**, 104815.
153 S. K. Hubadillah, M. R. Jamalludin, M. H. D. Othman and M. R. Adam, *Mater. Today Proc.*, 2023, DOI: **10.1016/j.matpr.2022.12.232**.
154 R. M. Anggraini, T. Restianingsih, F. Deswardani, Y. Fendriani and R. A. P. Purba, *J. Phys.*, 2023, **9**, 49–54.
155 A. Pramono, F. Sulaiman, S. Suryana, A. Alfirano and A. Milandia, *Mater. Sci. Forum*, 2020, **988**, 182–191.
156 A. D. Wuntu, D. M. H. Mantiri, J. J. H. Paulus and H. F. Aritonang, *AACL Bioflux*, 2021, **14**, 612–619.
157 S. Sridevi, S. Sutha, L. Kavitha and D. Gopi, *Mater. Chem. Phys.*, 2020, **254**, 123455.
158 T. P. Boaventura, A. M. Peres, V. S. B. Gil, C. S. B. Gil, R. L. Oréfice and R. K. Luz, *Quim. Nova*, 2020, **43**, 168–174.
159 G. Dorcioman, V. Grumezescu, G. E. Stan, M. C. Chifiriuc, G. P. Gradisteanu, F. Miculescu, E. Matei, G. Popescu-Pelin, I. Zgura, V. Craciun, F. N. Oktar and L. Duta, *Pharmaceutics*, 2023, **15**, 1294.
160 J. A. da Cruz, W. R. Weinand, A. M. Neto, R. S. Palácios, A. J. M. Sales, P. R. Prezas, M. M. Costa and M. P. F. Graça, *JOM*, 2020, **72**, 1435–1442.
161 S. M. Naga, H. F. El-Maghraby, E. M. Mahmoud, M. S. Talaat and A. M. Ibrhim, *Ceram. Int.*, 2015, **41**, 15010–15016.
162 E. S. Akpan, M. Dauda, L. S. Kuburi, D. O. Obada and D. Dodoo-Arhin, *Res. Phys.*, 2020, **17**, 103051.
163 P. Surya, A. Nithin, A. Sundaramanickam and M. Sathish, *J. Mech. Behav. Biomed. Mater.*, 2021, **119**, 104501.
164 M. Nag, A. Saffarzadeh, T. Nomichi, T. Shimaoka and H. Nakayama, *Waste Manag.*, 2020, **118**, 281–290.
165 P. Kusumawati, P. Triwitono, S. Anggrahini and Y. Pranoto, *Squal. Bull. Mar. Fish. Postharvest Biotechnol.*, 2022, **17**, 1–12.
166 P. L. Hariani, A. Rachmat, M. Said and S. Salni, *Indones. J. Chem.*, 2021, **21**, 1471–1483.
167 A. T. Idowu, S. Benjakul, S. Sinthusamran, T. Sae-leaw, N. Suzuki, Y. Kitani and P. Sookchoo, *Appl. Sci.*, 2020, **10**, 4141.
168 M. K. dos, S. Horta, C. Westin, D. N. da Rocha, J. B. de Campos, R. F. M. de Souza, M. S. Aguilar and F. J. Moura, *Mater. Res.*, 2023, **26**, e20220466.
169 A. F. Ahamed, M. Manimohan and N. Kalaivasan, *J. Inorg. Organomet. Polym.*, 2022, **32**, 3902–3922.
170 K. H. Le Ho, V. H. Dao, X. K. Pham, P. A. Nguyen, B. V. Phan, T. T. Doan and T. H. Lam, *Reg. Stud. Mar. Sci.*, 2022, **55**, 102560.
171 H. Yamamura, V. H. P. da Silva, P. L. M. Ruiz, V. Ussui, D. R. R. Lazar, A. C. M. Renno and D. A. Ribeiro, *J. Mech. Behav. Biomed. Mater.*, 2018, **80**, 137–142.
172 M. Bas, S. Daglilar, N. Kuskonmaz, C. Kalkandelen, G. Erdemir, S. E. Kuruca, D. Tulyaganov, T. Yoshioka, O. Gunduz, D. Ficai and A. Ficai, *Int. J. Mol. Sci.*, 2020, **21**, 8082.
173 M. Fitri, S. U. Tartar, S. Nurmiah and I. Syukroni, *Asian Food Sci. J.*, 2022, **21**, 78–85.
174 S. Boudreau, S. Hrapovic, Y. Liu, A. C. W. Leung, E. Lam and F. M. Kerton, *RSC Sustain.*, 2023, **1**, 1554–1564.
175 S. Boudreau, S. Hrapovic, E. McIsaac, E. Lam, F. Berrué and F. M. Kerton, *RSC Sustain.*, 2025, **3**, 2325–2332.
176 M. Fernández-Arias, I. Álvarez-Olcina, P. Malvido-Fresnillo, J. A. Vázquez, M. Boutinguiza, R. Comesaña and J. Pou, *Appl. Sci.*, 2021, **11**, 3387.
177 P. V. Nam, N. Van Hoa, T. T. L. Anh and T. S. Trung, *Waste Biomass Valorization*, 2020, **11**, 4195–4206.
178 Home, **https://nlmarineorganics.com/**, accessed August 14, 2025.
179 J. C. García-Santiago, C. J. Lozano Cavazos, J. A. González-Fuentes, A. Zermeño-González, E. Rascón Alvarado, A. Rojas Duarte, P. Preciado-Rangel, E. Troyo-Diéguez, F. M. Peña Ramos, L. A. Valdez-Aguilar, D. Alvarado-Camarillo and J. A. Hernández Maruri, *Biol. Agric. Hortic.*, 2021, **37**, 107–124.
180 W. Sun, M. H. Shahrajabian, Y. Kuang and N. Wang, *Plants*, 2024, **13**, 210.
181 D.-T. Van-Pham, V. V. Phat, N. H. Chiem, T. T. B. Quyen, N. T. N. Mai, D. H. Giao, T. N. Don and D. V. H. Thien, *Environ. Nat. Resour. J.*, 2022, **20**, 323–329.

© 2026 The Author(s). Published by the Royal Society of Chemistry

Open Access Article. Published on 10 ottobre 2025. Downloaded on 09/05/2026 05:18:07. This article is licensed under a Creative Commons Attribution-NonCommercial 3.0 Unported Licence.

182 M. K. dos, S. Horta, F. J. Moura, M. S. Aguilar, C. B. Westin, D. Navarro da Rocha and J. B. de Campos, *Int. J. Appl. Ceram. Technol.*, 2021, **18**, 1930–1937.
183 C. N. Aiza Jaafar, I. Zainol, M. I. Izyan Khairani and T. T. Dele-Afolabi, *Polymers*, 2022, **14**, 251.
184 B.-S. Liaw, T.-T. Chang, H.-K. Chang, W.-K. Liu and P.-Y. Chen, *J. Hazard. Mater.*, 2020, **382**, 121082.
185 P. Injorhor, T. Trongsatitkul, J. Wittayakun, C. Ruksakulpiwat and Y. Ruksakulpiwat, *Polymers*, 2022, **14**, 4158.
186 N. S. S. A. Buraiki, B. Ali Albadri, S. Alsheriqi, B. Alshabibi, S. Al-Mammari, S. Premkumar, M. K. Sah and M. S. Sudhakar, *Mater. Today Proc.*, 2020, **27**, 2609–2616.
187 M. Eswaran, S. Swamiappan, B. Chokkiah, R. Dhanusuraman, S. Bharathkumar and V. K. Ponnusamy, *Mater. Lett.*, 2021, **302**, 130341.
188 C. Sarkar and M. Das, *Indian J. Nat. Prod. Res.*, 2021, **12**, 359–368.
189 C.-S. Wu, S.-S. Wang, D.-Y. Wu and W.-L. Shih, *Addit. Manuf.*, 2021, **46**, 102169.
190 R. T. Rashad, *Acta Sci. Malays.*, 2023, **7**, 54–59.
191 M. A. Selimin, A. F. A. Latif, C. W. Lee, M. S. Muhamad, H. Basri and T. C. Lee, *Mater. Today Proc.*, 2022, **57**, 1142–1146.
192 A. Ashwitha, K. Thamizharasan and P. Bhatt, *SN Appl. Sci.*, 2020, **2**, 1228.
193 H. Wang, M. Qian, D. Zhang, Q. Wu and Z. Zhao, *Water*, 2023, **15**, 1274.
194 U. Sittitut, J. Jettanasen, S. Supothina and R. Rattanakam, *Inorganics*, 2022, **10**, 242.
195 M. O. de Amorim, J. C. C. S. Júnior, Y. L. Ruiz and J. C. S. Andrade, *Cerâmica*, 2021, **67**, 23–27.
196 P. Sricharoen, N. Limchoowong, P. Nuengmatcha and S. Chanthai, *Ultrason. Sonochem.*, 2020, **63**, 104966.
197 Y. Liu, J. Li, D. Wang, F. Yang, L. Zhang, S. Ji and S. Wang, *J. Food Sci.*, 2020, **85**, 150–156.
198 Y. Liu, M. Liu, S. Ji, L. Zhang, W. Cao, H. Wang and S. Wang, *Ceram. Int.*, 2021, **47**, 9366–9372.
199 O. Grahl-Nielsen and K. A. Glover, *Mar. Biol.*, 2010, **157**, 1567–1576.
200 S. Kongsri, K. Janpradit, K. Buapa, S. Techawongstien and S. Chanthai, *Chem. Eng. J.*, 2013, **215–216**, 522–532.
201 I. M. Savic and I. M. Savic Gajic, *J. Food Sci. Technol.*, 2020, **57**, 2809–2818.
202 M. M. Kininge and P. R. Gogate, *Ultrason. Sonochem.*, 2022, **82**, 105870.
203 M. Mofijur, F. Kusumo, I. M. R. Fattah, H. M. Mahmudul, M. G. Rasul, A. H. Shamsuddin and T. M. I. Mahlia, *Energies*, 2020, **13**, 1770.
204 E. Calcio Gaudino, G. Grillo, S. Tabasso, L. Stevanato, G. Cravotto, K. Marjamaa, V. Pihlajaniemi, A. Koivula, N. Aro, J. Uusitalo, J. Ropponen, L. Kuutti, P. Kivinen, H. Kanerva, A. Arshanitsa, L. Jashina, V. Jurkjane, A. Andersone, T. Dreyer and G. Schories, *J. Clean. Prod.*, 2022, **380**, 134897.
205 L. Liu, J. Li, J. Tian, Z. Zhou, J. Gao, L. Qin and J. Qiu, *Sustain. Chem. Pharm.*, 2024, **41**, 101718.
206 Q. Wang, L. Niu, J. Jiao, N. Guo, Y. Zang, Q. Gai and Y. Fu, *Biores. Technol.*, 2017, **244**, 969–974.
207 E. M. M. Flores, G. Cravotto, C. A. Bizzi, D. Santos and G. D. Iop, *Ultrason. Sonochem.*, 2021, **72**, 105455.
208 W.-K. Liu, B.-S. Liaw, H.-K. Chang, Y.-F. Wang and P.-Y. Chen, *JOM*, 2017, **69**, 713–718.
209 Q. Zhang, K. D. O. Vigier, S. Royer and F. Jérôme, *Chem. Soc. Rev.*, 2012, **41**, 7108–7146.
210 B. B. Hansen, S. Spittle, B. Chen, D. Poe, Y. Zhang, J. M. Klein, A. Horton, L. Adhikari, T. Zelovich, B. W. Doherty, B. Gurkan, E. J. Maginn, A. Ragauskas, M. Dadmun, T. A. Zawodzinski, G. A. Baker, M. E. Tuckerman, R. F. Savinell and J. R. Sangoro, *Chem. Rev.*, 2021, **121**, 1232–1285.
211 J. Afonso, A. Mezzetta, I. M. Marrucho and L. Guazzelli, *Green Chem.*, 2023, **25**, 59–105.
212 K. L. Hernández-Ruiz, J. López-Cervantes, D. I. Sánchez-Machado, M. D. R. Martínez-Macias, M. A. Correa-Murrieta and A. Sanches-Silva, *Sustain. Chem. Pharm.*, 2022, **28**, 100726.
213 L. Degli Esposti, A. C. Ionescu, S. Gandolfi, N. Ilie, A. Adamiano, E. Brambilla and M. Iafisco, *Dent. Mater.*, 2024, **40**, 593–607.
214 M. Boutinguiza, J. Pou, R. Comesaña, F. Lusquiños, A. de Carlos and B. León, *Mater. Sci. Eng., C*, 2012, **32**, 478–486.
215 L. Zhang, C. Zhang, R. Zhang, D. Jiang, Q. Zhu and S. Wang, *Mater. Lett.*, 2019, **236**, 680–682.
216 P. Acharya, M. Kupendra, A. Fasim, K. S. Anantharaju, N. Kottam, V. K. Murthy and S. S. More, *Biotechnol. Lett.*, 2022, **44**, 1175–1188.
217 P. Shi, M. Liu, F. Fan, C. Yu, W. Lu and M. Du, *Mater. Sci. Eng., C*, 2018, **90**, 706–712.
218 S. Righi, E. Prato, G. Magnani, V. Lama, F. Biandolino, I. Parlapiano, F. Carella, M. Iafisco and A. Adamiano, *Sci. Total Environ.*, 2023, **862**, 160751.
219 A. Adamiano, F. Carella, L. Degli Esposti, C. Piccirillo and M. Iafisco, *ACS Biomater. Sci. Eng.*, 2022, **8**, 4987–4995.
220 S. Parvin, Md. M. Hussain, F. Akter and B. K. Biswas, *J. Chem.*, 2021, **2021**, 9535644.
221 G. Falini, M. L. Basile, S. Gandolfi, F. Carella, G. Guarini, L. D. Esposti, M. Iafisco and A. Adamiano, *Ceram. Int.*, 2023, **49**, 243–252.
222 M. A. U. R. Al-Kazragi and D. T. A. Al-Heetimi, *J. Phys.: Conf. Ser.*, 2021, **1879**, 022073.
223 F. Mejbar, Y. Miyah, A. Lahrichi, S. Ssouni, A. Khalil, L. Nahali, M. Benjelloun, G. E. Mouhri and F. Zerrouq, *Moroccan J. Chem.*, 2021, **9**, 434–445.
224 Y. Miyah, M. Benjelloun, R. Salim, L. Nahali, F. Mejbar, A. Lahrichi, S. Iaich and F. Zerrouq, *J. Mol. Liq.*, 2022, **362**, 119739.
225 M. Nurhadi, R. Kusumawardani, W. Wirhanuddin, R. Gunawan and H. Nur, *Bull. Chem. React. Eng. Catal.*, 2019, **14**, 660–671.
226 T. S. Trung, N. C. Minh, H. N. Cuong, P. T. D. Phuong, P. A. Dat, P. V. Nam and N. V. Hoa, *J. Sci. Adv. Mater. Devices*, 2022, **7**, 100485.

© 2026 The Author(s). Published by the Royal Society of Chemistry

Open Access Article. Published on 10 ottobre 2025. Downloaded on 09/05/2026 05:18:07.
This article is licensed under a Creative Commons Attribution-NonCommercial 3.0 Unported Licence.

227 S. Swamiappan, S. Ganesan, V. Sekar, S. Devaraj, A. Subramanian, V. K. Ponnusamy and P. Kathirvel, *Int. J. Appl. Ceram. Technol.*, 2021, **18**, 902–912.
228 Md. A. Hossain, P. I. Turzo, Md. S. R. Shakil and F. Tuj-Zohra, *Water Pract. Technol.*, 2023, **18**, 2277–2295.
229 A. Nayak and B. Bhushan, *Mater. Today Proc.*, 2021, **46**, 11029–11034.
230 F. H. Jaffar, M. H. D. Othman, N. J. Ismail, M. H. Puteh, T. A. Kurniawan, S. Abu Bakar and H. Abdullah, *J. Taiwan Inst. Chem. Eng.*, 2024, **164**, 105668.
231 W. Yang, W. Luo, T. Sun, Y. Xu and Y. Sun, *Int. J. Environ. Res. Public Health*, 2022, **19**, 1260.
232 X. Qi, H. Yin, M. Zhu, X. Yu, P. Shao and Z. Dang, *Chemosphere*, 2022, **294**, 133733.
233 S. Mostofa, S. A. Jahan, B. Saha, N. Sharmin and S. Ahmed, *Environ. Nanotechnol. Monit. Manag.*, 2022, **18**, 100738.
234 H. M. Tauqeer, Z. Basharat, P. M. Adnan Ramzani, M. Farhad, K. Lewińska, V. Turan, A. Karczewska, S. A. Khan, G. Faran and M. Iqbal, *Environ. Pollut.*, 2022, **313**, 120064.
235 M. Nag, A. Saffarzadeh, T. Shimaoka and H. Nakayama, *Environ. Sci. Technol.*, 2022, **5**, 137–147.
236 N. Fijoł, H. Nasser Abdelhamid, B. Pillai, S. A. Hall, N. Thomas and A. P. Mathew, *RSC Adv.*, 2021, **11**, 32408–32418.
237 A. Saffarzadeh, M. Nag, T. Nomichi, T. Shimaoka, H. Nakayama and T. Komiya, in *Recent Advances in Environmental Science from the Euro-Mediterranean and Surrounding Regions*, ed. M. Ksibi, A. Ghorbal, S. Chakraborty, H. I. Chaminé, M. Barbieri, G. Guerriero, O. Hentati, A. Negm, A. Lehmann, J. Römbke, A. Costa Duarte, E. Xoplaki, N. Khélifi, G. Colinet, J. Miguel Dias, I. Gargouri, E. D. Van Hullebusch, B. Sánchez Cabrero, S. Ferlisi, C. Tizaoui, A. Kallel, S. Rtimi, S. Panda, P. Michaud, J. N. Sahu, M. Seffen and V. Naddeo, Springer Int. Publ., Cham, 2nd edn, 2021, pp. 789–794.
238 N. V. Hoa, N. C. Minh, H. N. Cuong, P. A. Dat, P. V. Nam, P. H. T. Viet, P. T. D. Phuong and T. S. Trung, *Molecules*, 2021, **26**, 6127.
239 M. N. Rashed, A. A. E. Gad and N. M. Fathy, *Biomass Convers. Biorefinery*, 2024, **14**, 31703–31720.
240 M. Khanjani, D. J. Westenberg, A. Kumar and H. Ma, *ACS Omega*, 2021, **6**, 11988–12003.
241 M. Ghattas, A. Chevrier, D. Wang, M.-G. Alameh and M. Lavertu, *Carbohydr. Polym. Technol. Appl.*, 2025, **10**, 100797.

© 2026 The Author(s). Published by the Royal Society of Chemistry